[redacted]

NASA TECHNICAL MEMORANDUM

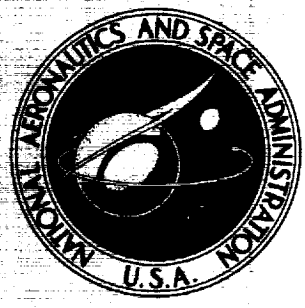

UB
NASA TM X-1588

[redacted]

UB
NASA TM X-1588

FULL-SCALE WIND-TUNNEL INVESTIGATION OF THE AERODYNAMIC CHARACTERISTICS OF THE M2-F2 LIFTING BODY FLIGHT VEHICLE

by Kenneth W. Mort and Berl Gamse

Ames Research Center
Moffett Field, Calif.

NATIONAL AERONAUTICS AND SPACE ADMINISTRATION • WASHINGTON, D. C. • JUNE 1968

[redacted]

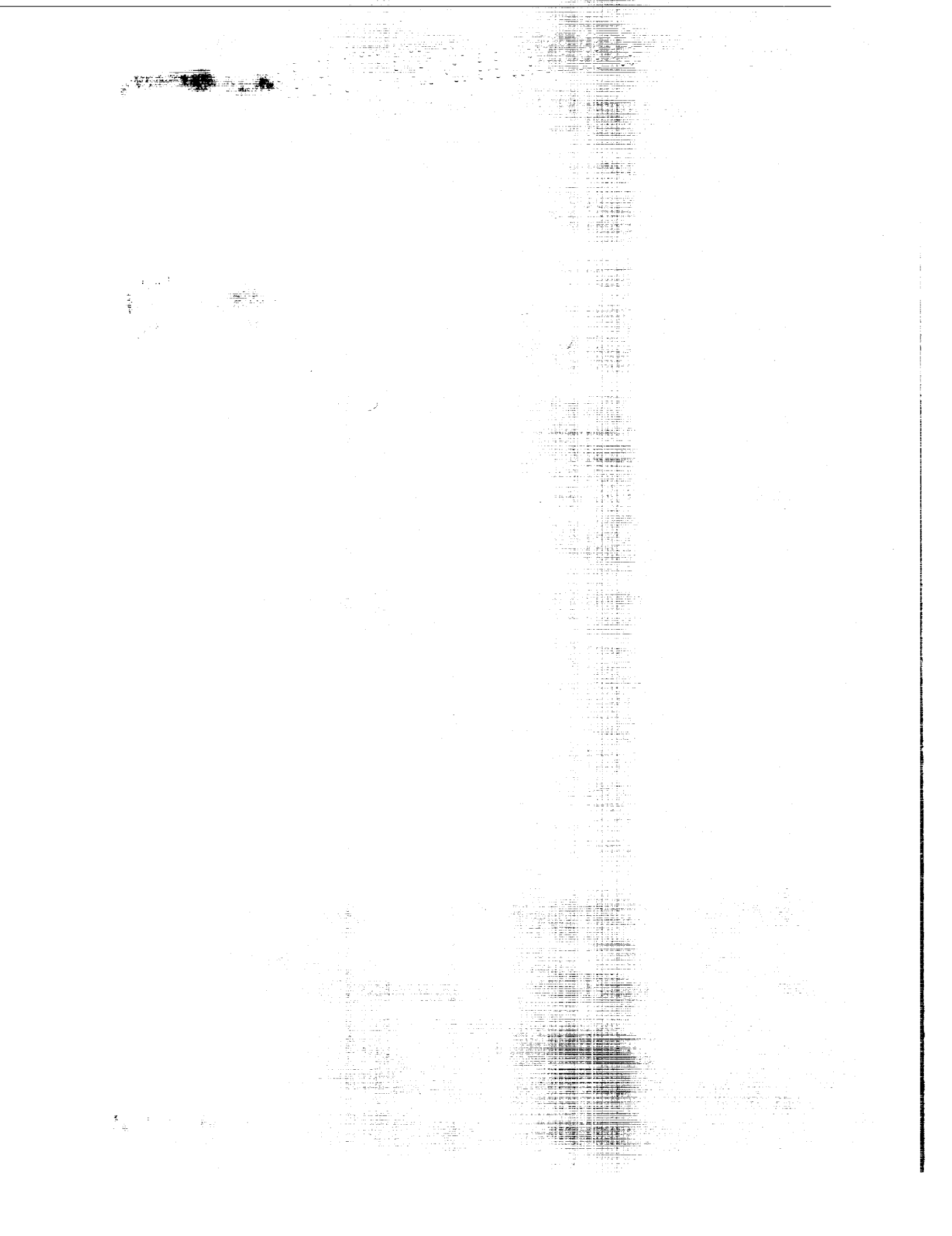

[redacted]

NASA TM X-1588

[redacted]

FULL-SCALE WIND-TUNNEL INVESTIGATION OF THE AERODYNAMIC CHARACTERISTICS OF THE M2-F2 LIFTING BODY FLIGHT VEHICLE

By Kenneth W. Mort and Berl Gamse

Ames Research Center
Moffett Field, Calif.

[redacted]

NATIONAL AERONAUTICS AND SPACE ADMINISTRATION

[redacted]

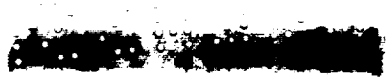

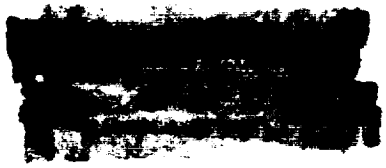

[redacted]

FULL-SCALE WIND-TUNNEL INVESTIGATION OF THE AERODYNAMIC CHARACTERISTICS OF THE M2-F2 LIFTING BODY FLIGHT VEHICLE*

By Kenneth W. Mort and Berl Gamse

Ames Research Center

SUMMARY

The aerodynamic characteristics of the M2-F2 flight vehicle were investigated in the Ames 40- by 80-foot wind tunnel. The vehicle was tested over an angle-of-attack range of -10° to $+28^{\circ}$, an angle-of-sideslip range of -5° to $+10^{\circ}$, for several longitudinal, lateral, and directional control settings, and for Reynolds numbers ranging from 20.3×10^{6} to 37.5×10^{6}. Results were obtained with the landing gear both up and down. The maximum lift-to-drag ratio achieved was 3.7 untrimmed and 3.5 trimmed. The presence of the landing gear reduced the L/D by about 1 and during flight would require a longitudinal control change of 2° to 5°, depending on the angle of attack, to maintain a constant angle of attack or forward velocity. A comparison was made between wind-tunnel and flight determined results and good agreement was shown.

INTRODUCTION

Many studies have been conducted in developing lifting reentry configurations capable of gliding to a specified recovery site and making a horizontal landing. One of these configurations is the M2 lifting body. Wind-tunnel and flight investigations have been performed on the first M2 flight vehicle designated the M2-F1 (see refs. 1 and 2). This vehicle was designed and constructed for flight investigations in the low-speed regime of the flare and landing maneuver. The M2-F2 was developed to investigate flying qualities at the higher flight velocities which would be encountered prior to the landing maneuver. The M2-F2 employed riveted sheetmetal skin construction while the M2-F1 employed sailplane type plywood skin construction. There were major differences in the control system, and a boattail fairing was added to the M2-F2.

Low-speed aerodynamic characteristics of the M2-F2 configuration, initially determined from wind-tunnel investigations of a full-scale wind-tunnel model, are reported in reference 3. To ensure that the differences between the low-speed aerodynamic characteristics of the full-scale model and the flight vehicle due to small physical differences would not be unacceptably large, the flight vehicle was tested in the Ames 40- by 80-foot wind tunnel prior to flight tests. Results of this investigation are presented herein.

---

*Title, Unclassified

[redacted]

NOTATION

b	reference span (maximum width without boattail), 9.51 ft
C_D	drag coefficient, $\frac{D}{qS}$
C_l	rolling-moment coefficient, $\frac{\text{rolling moment}}{qSb}$
C_L	lift coefficient, $\frac{L}{qS}$
C_m	pitching-moment coefficient, $\frac{\text{pitching moment}}{qSl}$
C_n	yawing-moment coefficient, $\frac{\text{yawing moment}}{qSb}$
C_y	side-force coefficient, $\frac{\text{side force}}{qS}$
D	drag force, lb
l	reference length (length excluding boattail), 20 ft
L	lift force, lb
q	free-stream dynamic pressure, psf
S	reference area, planform area excluding boattail, 138.9 ft^2
R	Reynolds number, $\frac{\text{free-stream velocity}}{\text{kinematic viscosity}}\, l$
α	angle of attack, upper surface used as the reference, deg
β	angle of sideslip, deg
δ_a	differential upper flap deflection ($\delta_{u_{left}} - \delta_{u_{right}}$), deg
δ_u	upper flap deflection, $\frac{1}{2}$ ($\delta_{u_{left}} + \delta_{u_{right}}$), deg
δ_l	lower flap deflection, deg
δ_r	rudder deflection ($\delta_{r_{left}} + \delta_{r_{right}}$), deg
δ_{rf}	rudder flare, $\frac{1}{2}$ ($\delta_{r_{left}} - \delta_{r_{right}} - \lvert\delta_r\rvert$), deg

The data presented are referred to the wind axis for all force coefficients and to the body axis for all moment coefficients.

The control surface deflections are defined in figure 1.

[redacted]

VEHICLE DESCRIPTION

The M2-F2 flight vehicle is shown in figure 2 installed in the test section of the Ames 40- by 80-foot wind tunnel. Dimensions and geometry are given in figure 3. The control system (figs. 1 and 3) included upper flaps that move together for longitudinal control and differentially for lateral control, and a lower flap which could be used independently or in conjunction with the upper flaps for longitudinal control. The lower flap was limited to a minimum deflection of 10°. As shown in figure 3(b) the vehicle had split flap type rudders on the outboard surfaces of the vertical stabilizers; only one surface at a time deflected outboard for directional control.

TEST PROCEDURE

The aerodynamic characteristics were obtained for various angles of attack or control positions at fixed dynamic pressures and sideslip angles. The effects of Reynolds numbers from 20.3×10^{6} to 37.5×10^{6} were determined at one longitudinal control setting and zero sideslip. Unless otherwise noted on the figures, the investigation was performed at a Reynolds number of 34×10^{6} (dynamic pressure of 83 psf).

REDUCTION OF DATA

Corrections

No tunnel-wall corrections were applied to the data presented since the estimated magnitude of these corrections indicated that they were insignificant.

The data were corrected for tares due to the unshielded strut tips. These tares were obtained without the vehicle on the struts. Errors from differences due to interaction with the vehicle should be small because of the manner in which the vehicle was mounted on the struts. The strut tips were long and narrow, and were positioned so that their wake would not impinge on the control surfaces. (See fig. 2.) With the landing gear up the tare values used were: drag coefficient, 0.014, and pitching-moment coefficient, -0.00278; with the landing gear down the values were: drag coefficient, 0.014, and pitching-moment coefficient, -0.00444.

Accuracy of Measurement

The various quantities measured were accurate within the following limits which include error limits involved in calibrating, reading, and reducing the data.

[redacted]

[redacted]

Angle of attack	$\pm 0.2^{\circ}$
Angle of sideslip	$\pm 0.3^{\circ}$
Lift	±10 lb
Drag	±3 lb
Side force	±3 lb
Pitching moment	±300 ft-lb
Yawing moment	±100 ft-lb
Rolling moment	±400 ft-lb
Free-stream dynamic pressure	±1/2 percent
Control surface settings	$\pm 0.3^{\circ}$

RESULTS AND DISCUSSION

Longitudinal Aerodynamic Characteristics

Basic results.- Results for several Reynolds numbers are shown in figure 4. For the range investigated the effect of Reynolds number on the forces was insignificant, but the effect on pitching moment was significant, and at the lower Reynolds number, would be sufficient to cause about a 4° error in predicted trim angle of attack. To minimize this discrepancy most of the results were obtained at higher Reynolds numbers ($R = 34 \times 10^6$, dynamic pressure of 83 psf).

Results for several longitudinal control settings with the landing gear both up and down are shown in figures 5 through 8. A comparison of figures 5 and 6 shows a nonlinear variation in pitching-moment coefficient with lift coefficient between about 8° and 12° angle of attack with the landing gear up but not with the gear down. This discrepancy is considered reasonable because of the size of the covers on the landing gear wells (see figs. 2(a) and (c)) and the effects that the covers and openings could have on the airflow over the vehicle.

Figure 9 shows the effect of rudder flare (symmetrical deflection of the rudders) on the longitudinal aerodynamic characteristics. The purpose of flaring the rudders is to control drag and, hence, glide path. It is evident that increased rudder flare caused significant increases in the drag coefficient as was intended; however, flaring the rudders also caused large decreases in pitching-moment coefficient (more nose down). This nose-down pitching moment would necessitate retrimming the vehicle to prevent an increase in velocity. (Rudder flare data were also obtained for longitudinal control settings of $\delta_u = 0^{\circ}$, $\delta_l = 20^{\circ}$ and $\delta_u = -10^{\circ}$, $\delta_l = 40^{\circ}$ with the landing

[redacted]

[redacted]

gear down. The variations in the aerodynamic characteristics with rudder flare were not different from those at $\delta_u = -10^\circ$, $\delta_l = 20^\circ$; hence these data are not included.)

Figures 10(a) and (b) show the effect of sideslip on the longitudinal aerodynamic characteristics with the landing gear up and down, respectively. With the landing gear up large variations in C_m due to sideslip occur between angles of attack of 0° and 16°. With the landing gear down, variations due to sideslip are small except at high angles of attack. These results suggest that the flow conditions which caused the nonlinear variations in C_m with the landing gear up were affected by sideslip.

Comparison with full-scale wind-tunnel model of reference 3.- The longitudinal aerodynamic characteristics of the flight vehicle (from fig. 5(c)) and full-scale model (from ref. 3) were compared to determine the effects on the aerodynamic characteristics of the small physical differences in smoothness, shape, camber, canopy, control surfaces, etc. The results are shown in figure 11. As can be seen there are significant differences. The minimum drag coefficient of the flight vehicle is larger by 0.015. For a given lift coefficient the angle of attack of the flight vehicle is lower by $1\text{-}1/2^\circ$ to 3°. In addition to these differences, there is a difference in pitching-moment coefficient at lift coefficients larger than about 0.55. For these conditions the pitching-moment coefficient for the flight vehicle is less (more nose down) than that for the full-scale model by values greater than 0.01, which is equivalent to an increment in lower flap deflection of about 5°. It may be concluded from these results that small differences in the physical characteristics caused significant differences in the aerodynamic characteristics.

Trimmed aerodynamic characteristics for the M2-F2 flight vehicle.- These results were obtained from the data in figures 7 and 8 and are presented in figure 12. The maximum trimmed lift-to-drag ratio (L/D) achieved was 3.5 with the landing gear up and 2.5 with the landing gear down. A comparison with the untrimmed values of 3.7 and 2.7 (figs. 5 and 6) indicates that the trim drag reduced the maximum L/D by 0.2.

Deploying the landing gear not only reduced L/D but caused a nose-down change in pitching moment (cf. figs. 12(a) and (b)). This change would necessitate a 2° to 5° change in the lower flap deflection, depending on the angle of attack, to retrim the vehicle at the same angle of attack or lift coefficient.

Comparison of the wind-tunnel results with the flight determined results from reference 4.- During flight, the vehicle center of gravity was at the 130.5-inch station instead of the 132-inch station, and the rudders were set at 5° of flare instead of 0°. The data of figure 7 were recomputed using the flight moment reference and corrected for the 5° of rudder flare. (The following increments determined from the data in figure 9 were added to the data of figure 7 to correct for the rudder flare: $\Delta C_L = 0.004$, $\Delta C_D = 0.009$, $\Delta C_m = -0.006$.) From these results trim data were determined and are compared in figure 13 with the flight data from reference 4.

[redacted]

As can be seen from figure 13 there are small differences in the lift and drag data which result in a net difference in maximum L/D of about 0.2; the wind-tunnel value is lower than that from flight. The most significant difference is in the control position required for a given angle of attack. The lower flap deflection is 2° to 3° less for the wind tunnel determined results than it is for the flight determined results for angles of attack between -4° and $+8^\circ$.

Generally, the agreement between the data from flight and from the wind-tunnel tests was considered good, especially in view of the following differences in test conditions.

a. During the flight tests the Mach number was substantially higher than it was during the wind-tunnel tests.

b. During the wind-tunnel tests the struts could have introduced small unaccounted for errors in C_L, C_D, α, and C_m.

c. During flight tests the vehicle did not have the box fairing between the lower flap and body shown in figure 3.

d. During the flight tests the control position data were not corrected to trim conditions, but this effect should be small.

Lateral-Directional Aerodynamic Characteristics

These results are presented in figures 14 through 16. Figure 14 shows the effects of sideslip, figure 15 the effects of directional control, and figure 16 the effects of roll control. Results for only one longitudinal control setting are presented because different longitudinal control settings did not affect these results for the ranges tested (δ_u from 0° to -35° and δ_l from 10° to 45°). In addition, data for roll control with the landing gear down are not presented because the presence of the landing gear did not affect these data.

The significant features which should be noted from the lateral-directional data are the following. Comparison of figures 14(a) and 14(b) indicates that the presence of the landing gear caused a decrease in C_{y_β} of about 60 percent and an increase in C_{l_β} of about 20 percent at low angles of attack. Comparison of the results of figure 15(a) for the two flare positions indicates that 20° of rudder flare reduced the directional control effectiveness about 30 percent. Figure 16 shows a large adverse yawing moment with roll control ($C_{n_{\delta_a}}/C_{l_{\delta_a}} \approx -1$). This was also evident from the investigation of reference 3. A method of reducing the magnitude of ($C_{n_{\delta_a}}/C_{l_{\delta_a}}$) was discussed in this reference.

SUMMARY OF RESULTS

The maximum L/D achieved was 3.7 untrimmed and 3.5 trimmed.

The landing gear caused the following effects:

a. A 2° to 5° control flap change to retrim the vehicle and maintain the angle of attack or lift coefficient, depending on the angle of attack.

b. A reduction in $(L/D)_{max}$ of about 1.

c. A decrease in C_{y_β} of about 60 percent and an increase in C_{l_β} of about 20 percent for low angles of attack.

The pitching-moment coefficient varied nonlinearly with lift coefficient between α values of 8° and 12°. This nonlinearity occurred only with the landing gear up and appeared to be affected by sideslip.

The longitudinal results obtained from testing the flight vehicle were compared with those obtained from testing the full-scale wind-tunnel model of reference 3. This comparison indicated significant differences; hence the advisability of testing the actual flight vehicle rather than relying on tests of wind-tunnel models is apparent.

The wind tunnel determined aerodynamic characteristics agreed well with flight determined results. This agreement was better than that between the wind-tunnel model and flight vehicle.

Ames Research Center
National Aeronautics and Space Administration
Moffett Field, Calif., Feb. 27, 1968
124-07-02-10-00-21

[redacted]

REFERENCES

1. Mort, Kenneth W.; and Gamse, Berl: Full-Scale Wind-Tunnel Investigation of the Longitudinal Aerodynamic Characteristics of the M2-F1 Lifting Body Flight Vehicle. NASA TN D-3330, 1966.

2. Horton, Victor W.; Eldredge, Richard C.; and Klein, Richard E.: Flight-Determined Low-Speed Lift and Drag Characteristics of the Lightweight M2-F1 Lifting Body. NASA TN D-3021, 1965.

3. Mort, Kenneth W.; and Gamse, Berl: Low-Speed Wind-Tunnel Tests of a Full-Scale M2-F2 Lifting Body Model. NASA TM X-1347, 1967.

4. Pyle, Jon S.; and Swanson, Robert H.: Lift and Drag Characteristics of the M2-F2 Lifting Body During Subsonic Gliding Flight. NASA TM X-1431, 1967.

[redacted]

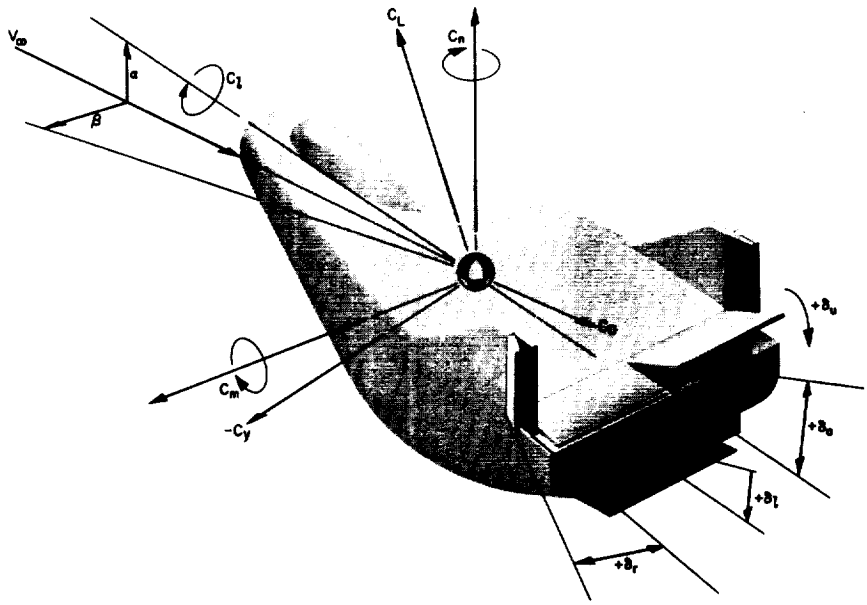

Figure 1.- Sign conventions.

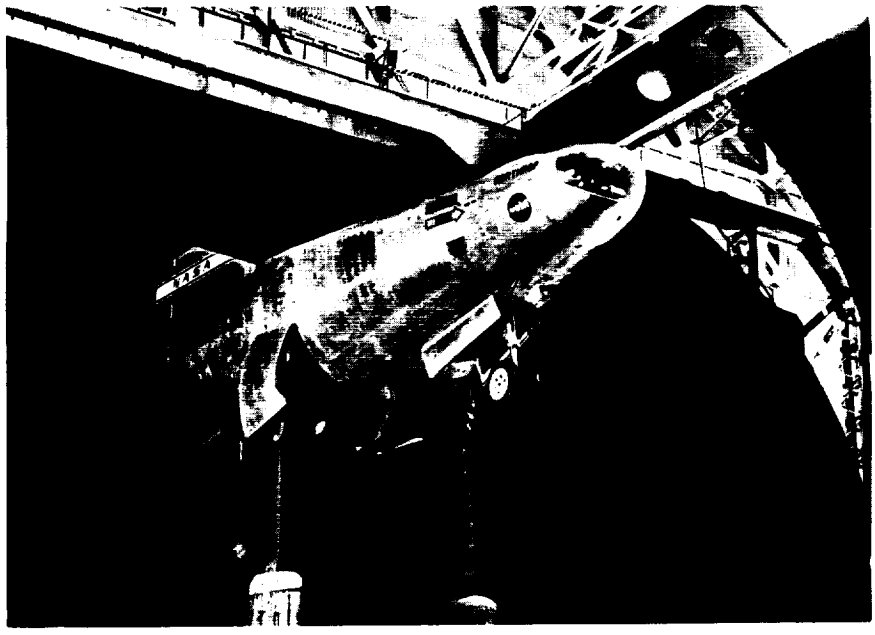

A-35069

(a) Three-quarter front view with landing gear down.

Figure 2.- Vehicle mounted in the Ames 40- by 80-Foot Wind Tunnel.

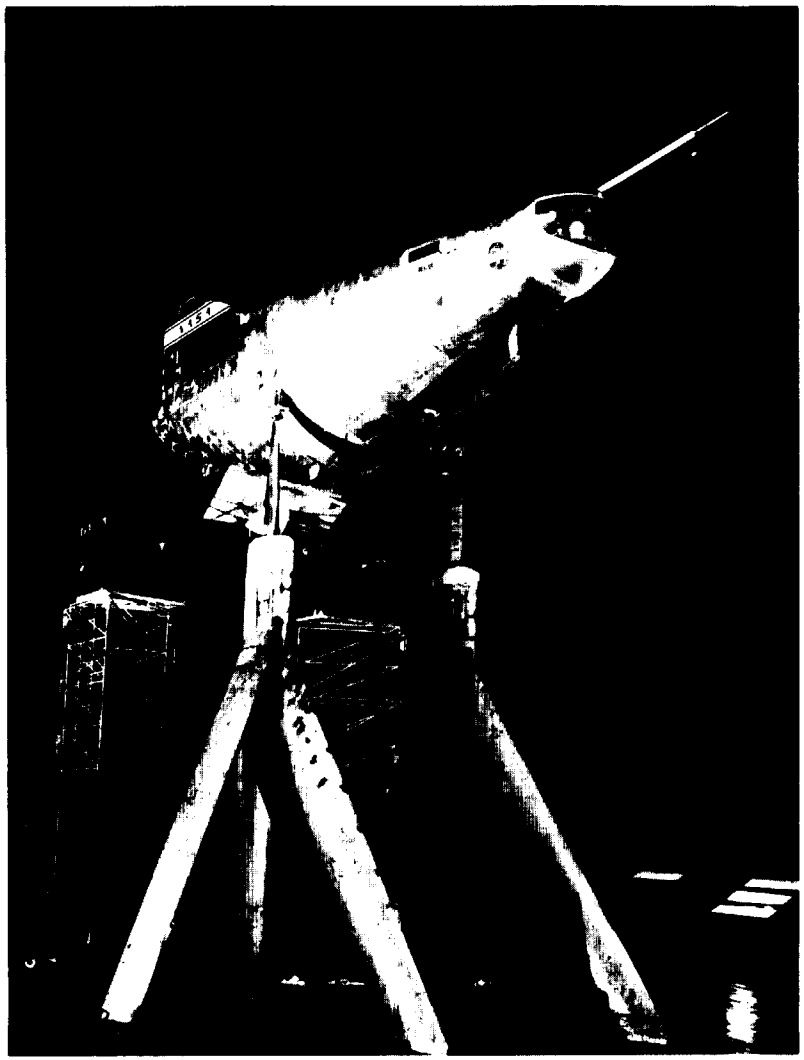

A-35070

(b) Three-quarter front view.

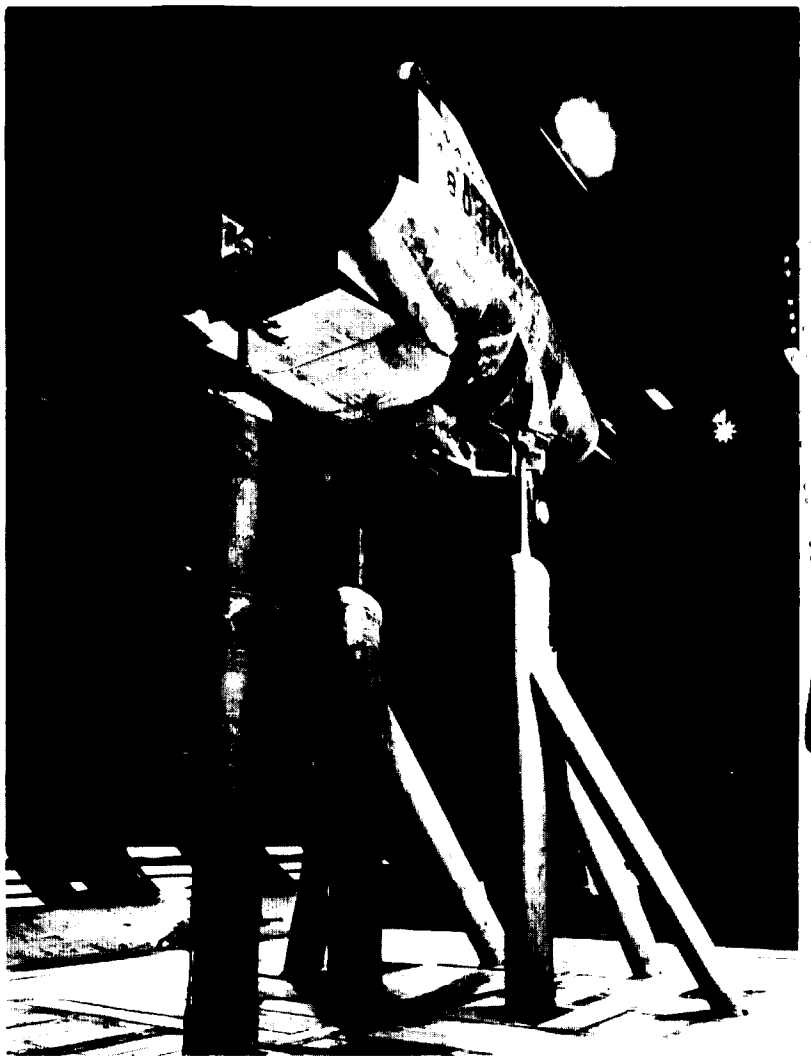

A-35072

(c) Three-quarter rear view with landing gear down.

Figure 2.- Concluded.

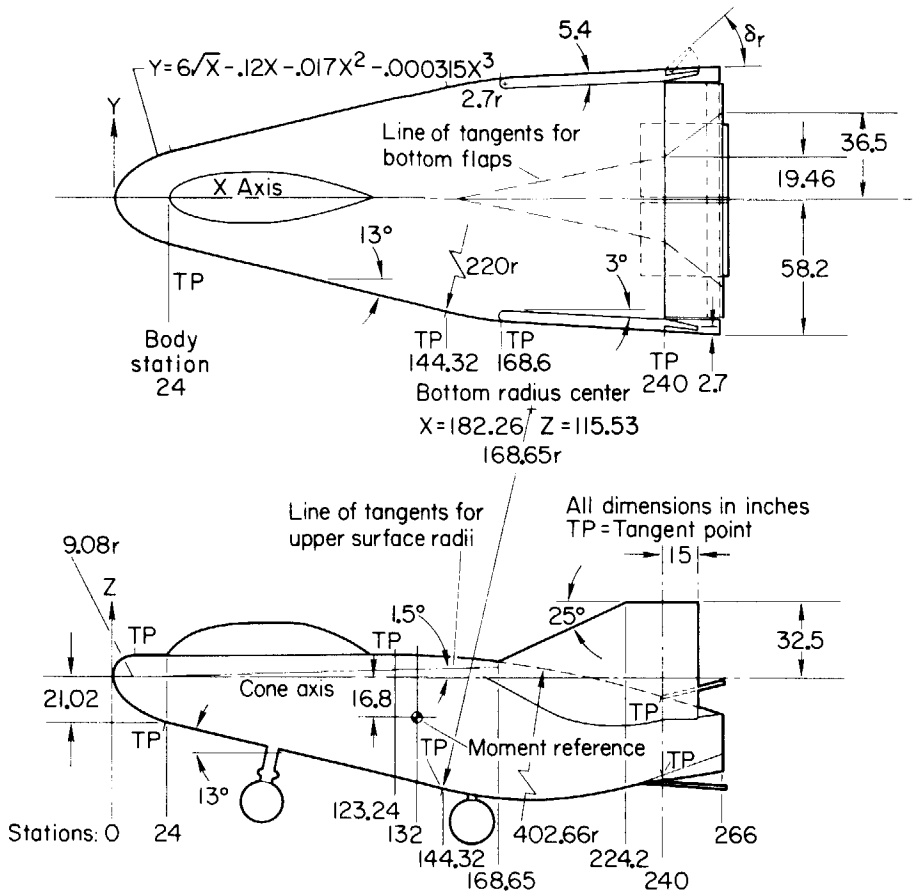

Canopy coordinates

Station inches	Y inches	Z - 9.08 inches
24	0	0
29	5.85	5.85
32	9.45	10.90
49	10.75	13.25
59	11.10	14.00
69	10.90	14.00
79	9.75	14.00
89	7.65	12.00
99	4.85	8.00
109	1.25	2.40
111.5	0	0

Top of canopy is composed of circular cross sections.

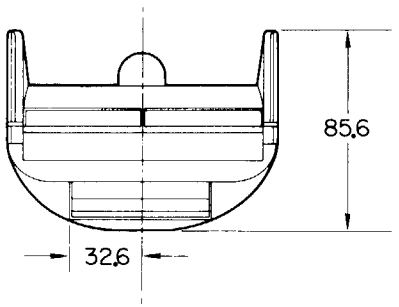

(a) Basic dimensions.

Figure 3.- Model dimensions.

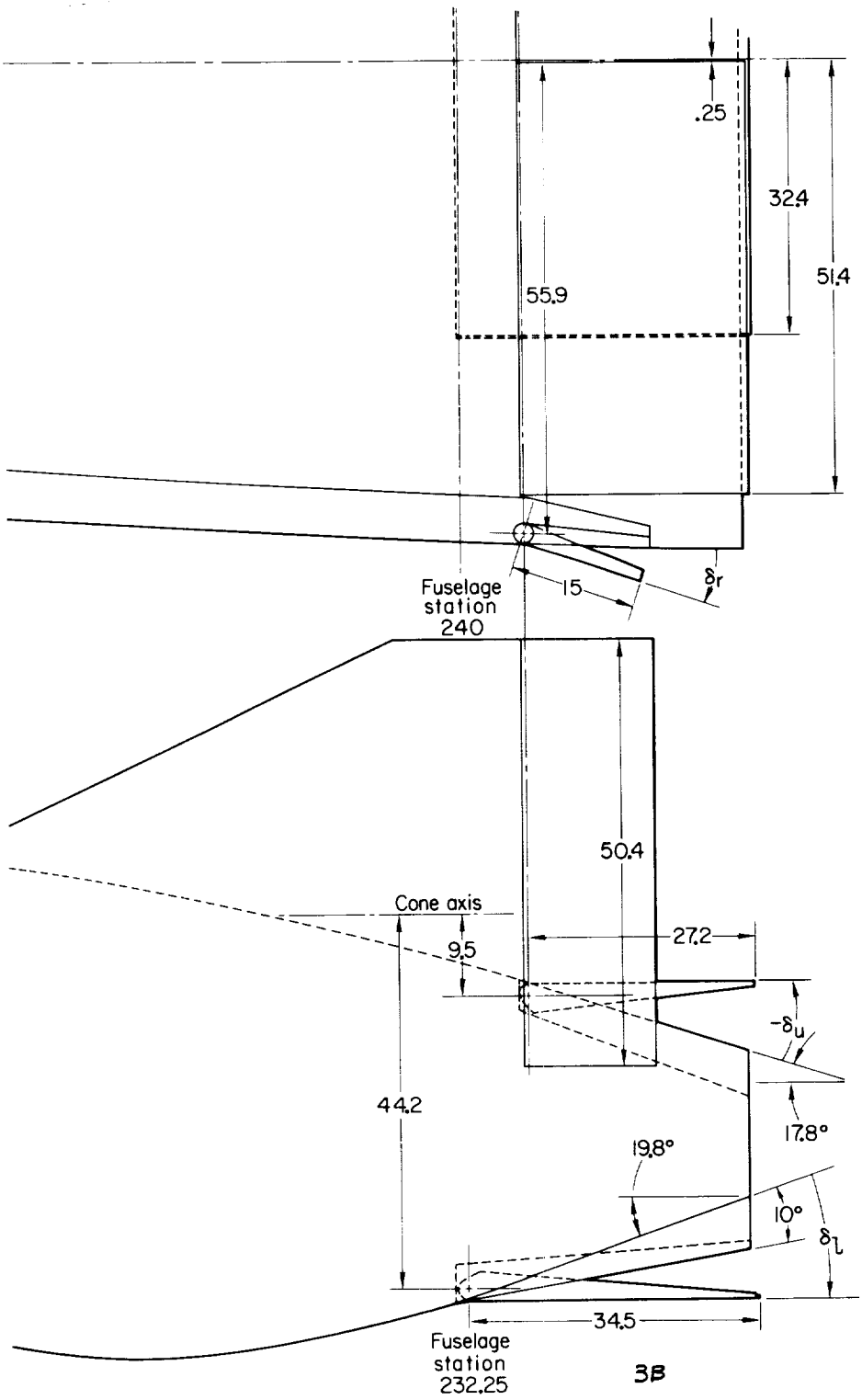

(b) Details of control surfaces.

Figure 3.- Concluded.

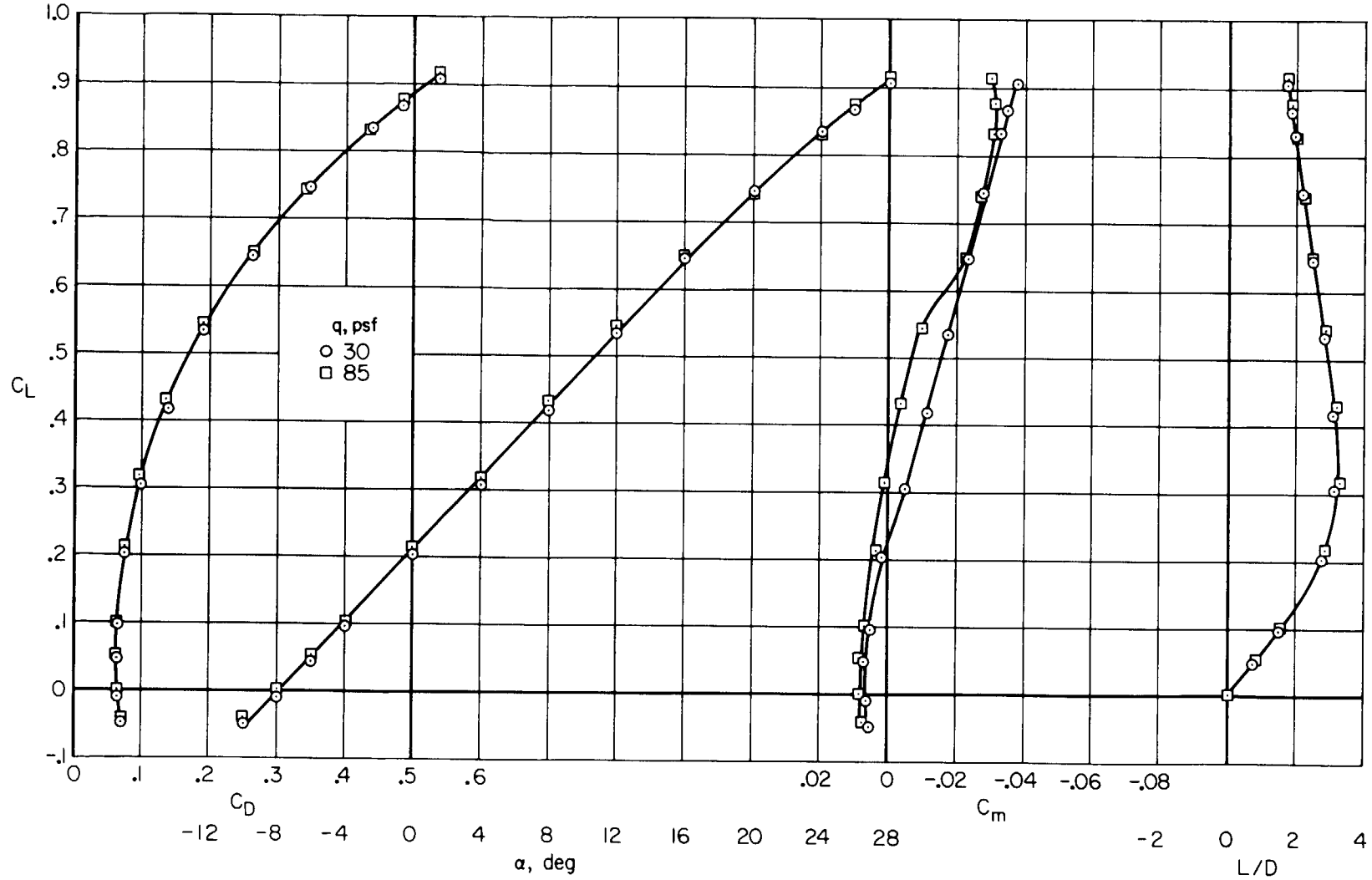

(a) Landing gear up.

Figure 4.- Effect of dynamic pressure on longitudinal aerodynamic characteristics; $-\delta_u = -10^\circ$, $\delta_l = 20^\circ$.

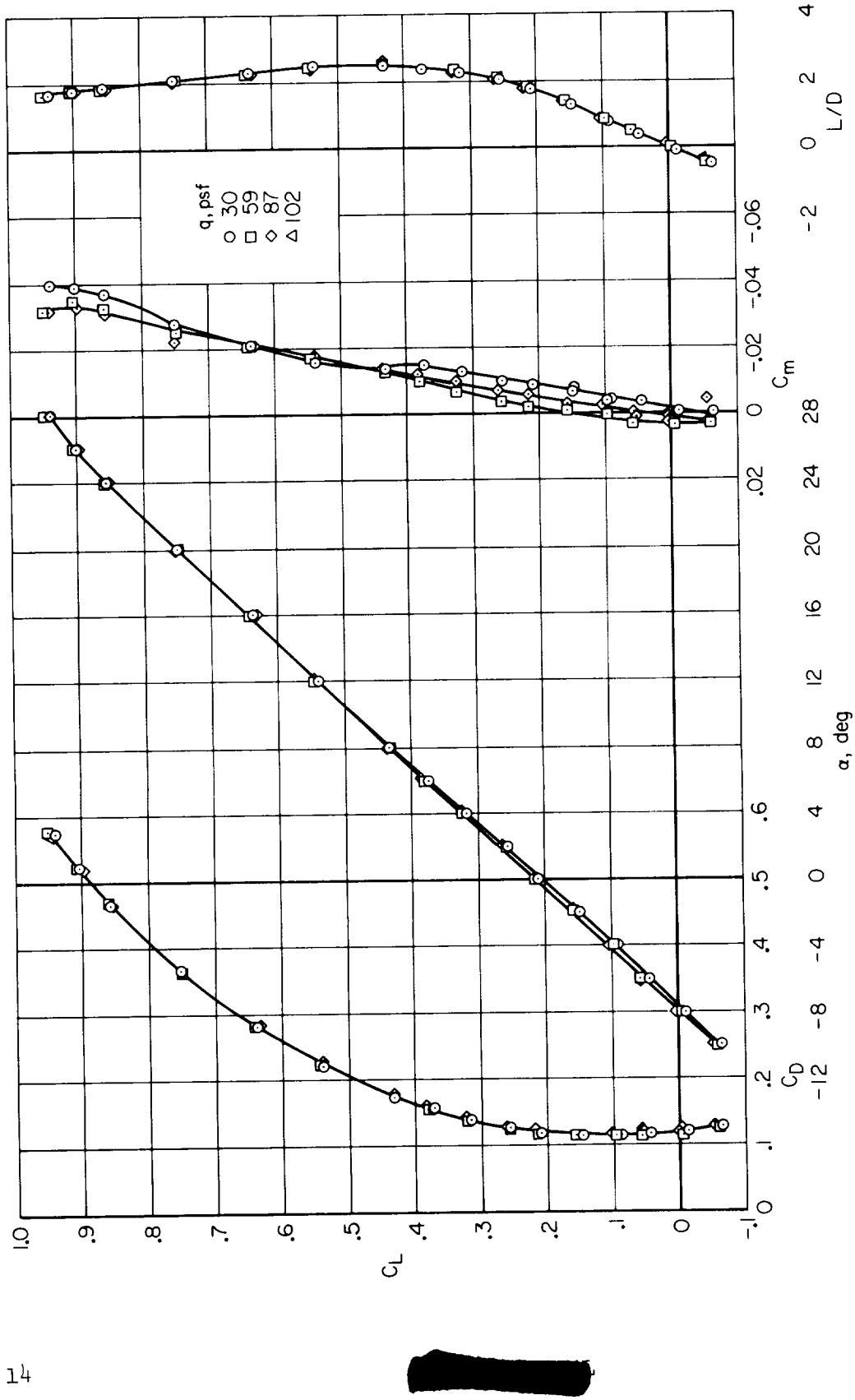

(b) Landing gear down.

Figure 4.- Concluded.

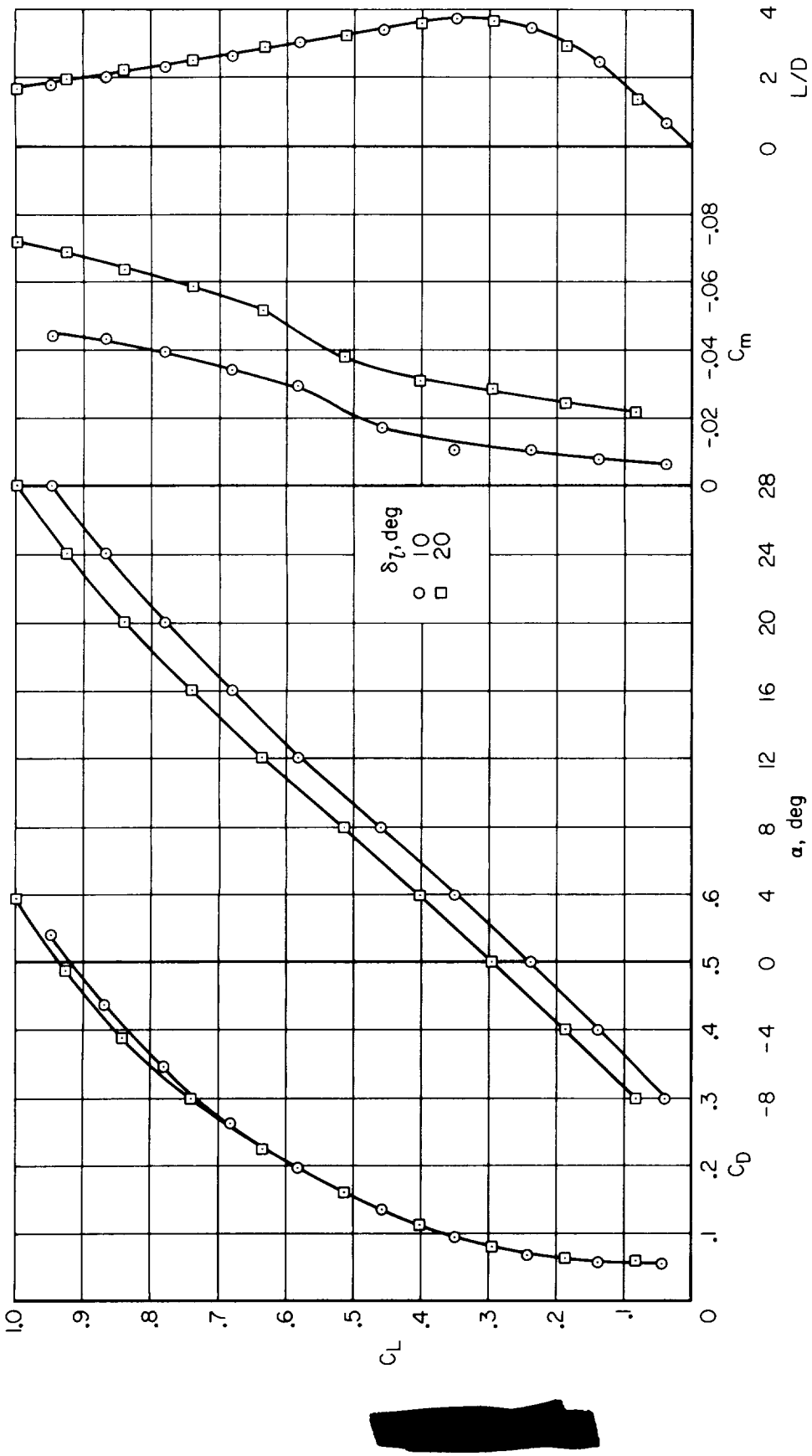

(a) $\delta_u = 0^\circ$

Figure 5.- Longitudinal aerodynamic characteristics for several control settings with the landing gear up.

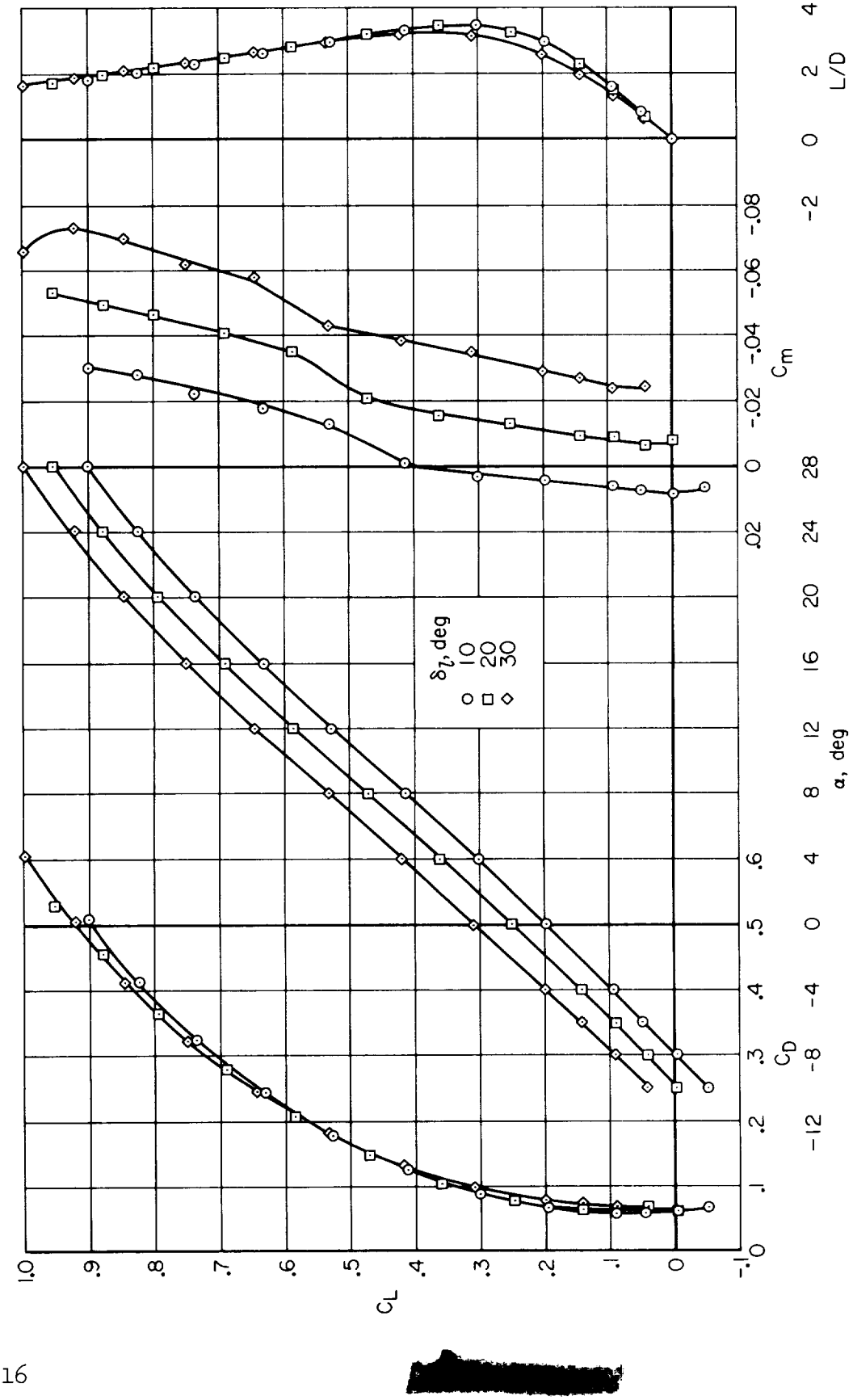

(b) $\delta_u = -5^\circ$

Figure 5.- Continued.

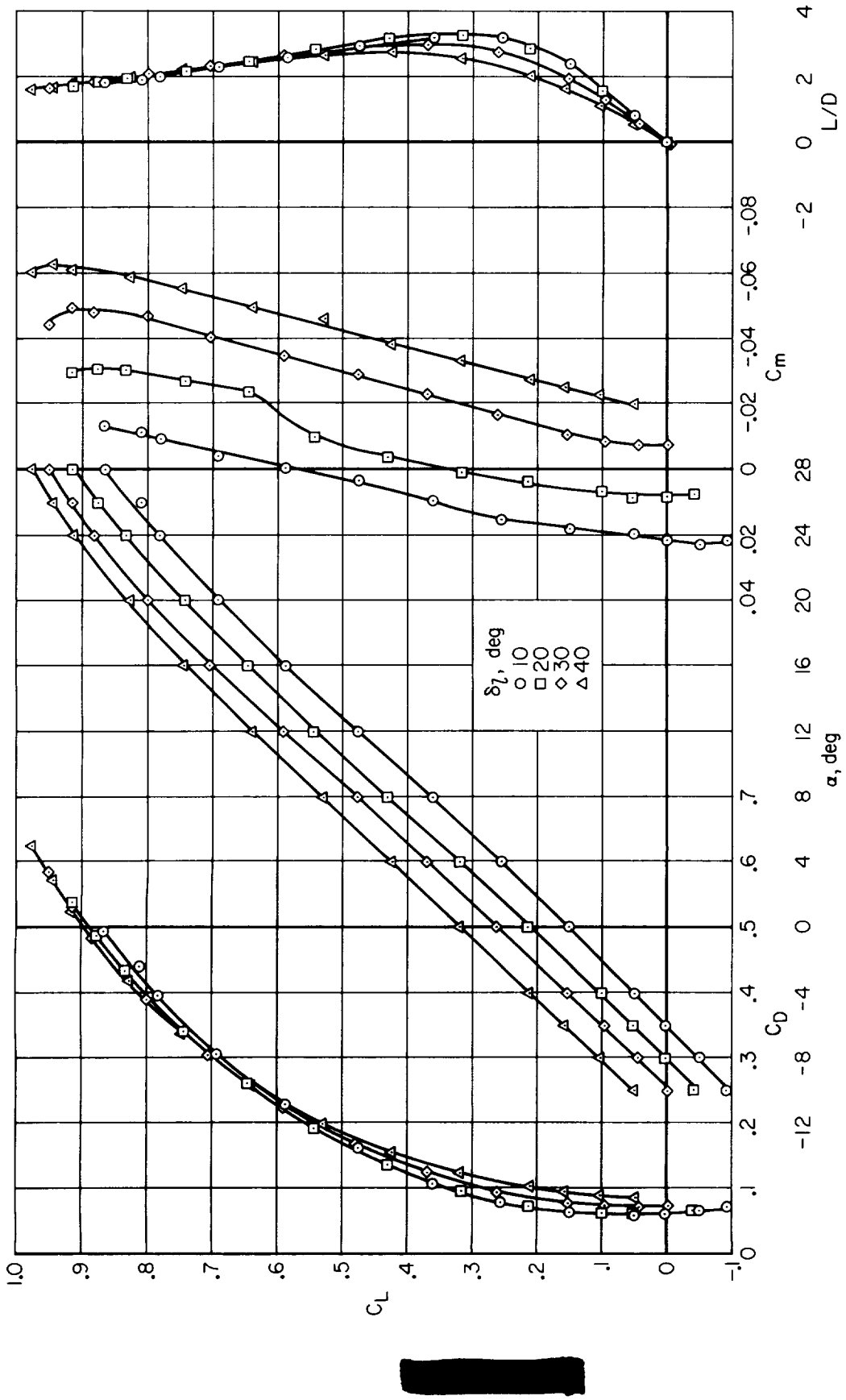

(c) $\delta_u = -10^\circ$

Figure 5.- Continued.

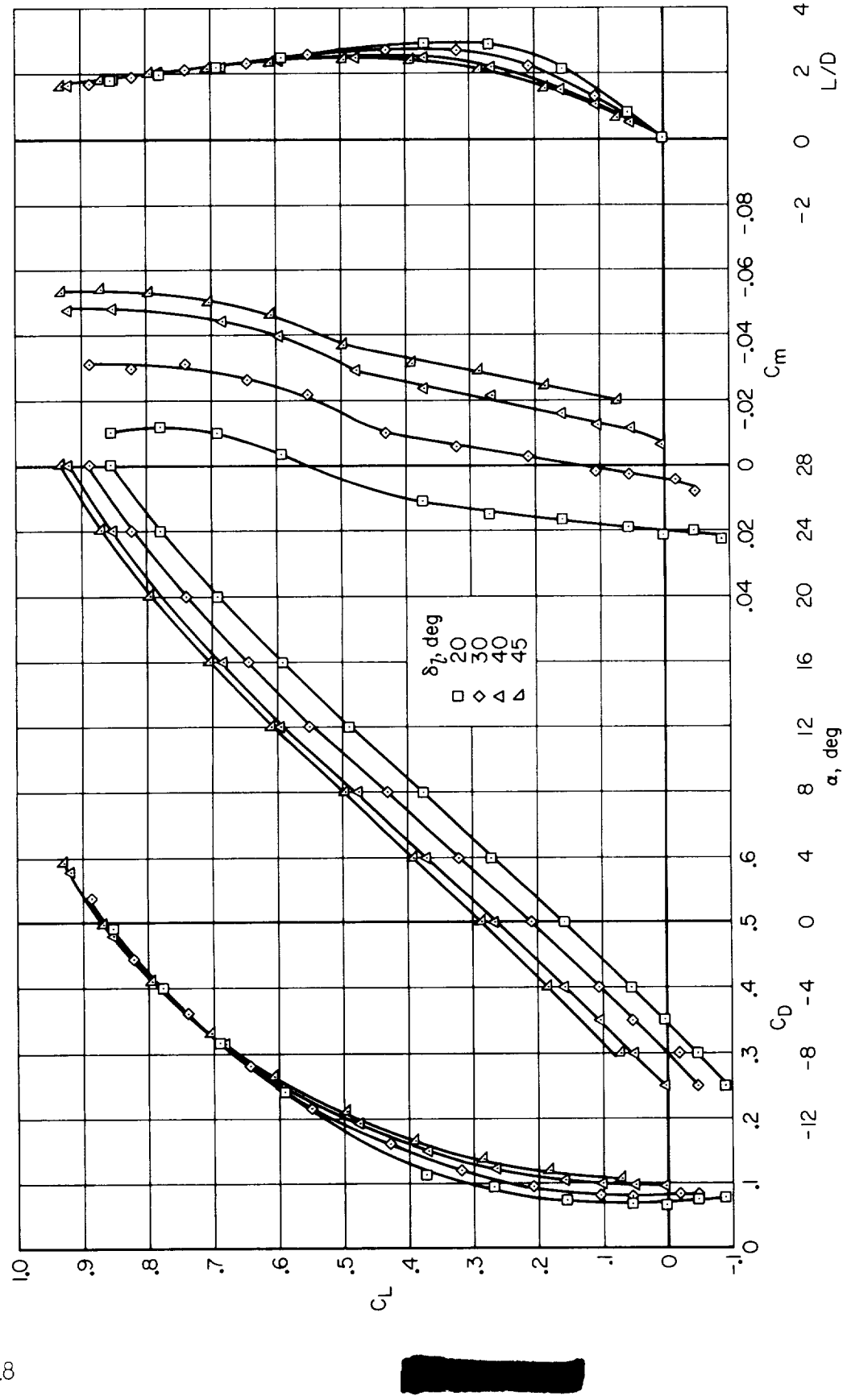

(d) $\delta_u = -15^\circ$

Figure 5.- Continued.

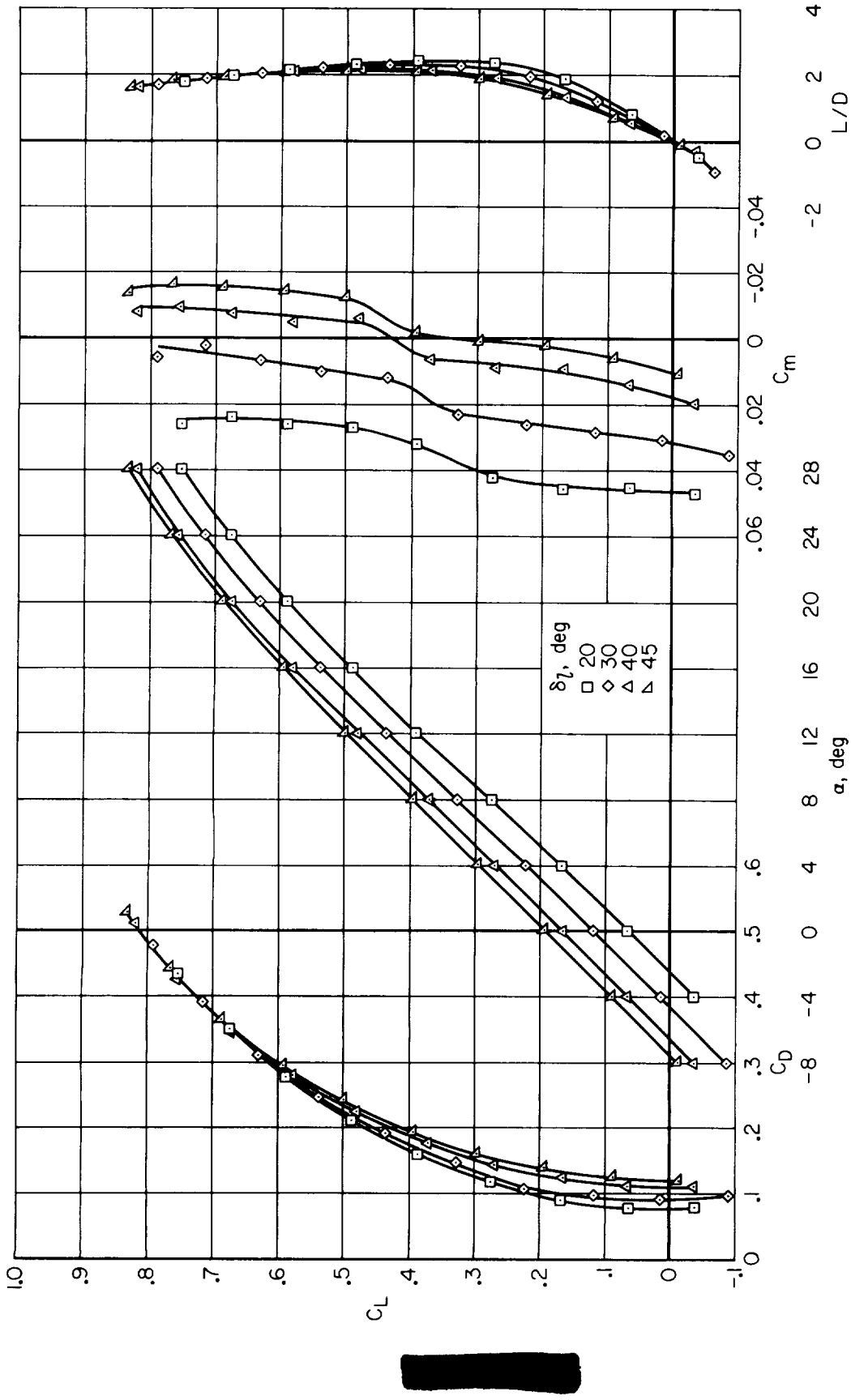

(e) $\delta_u = -25^\circ$

Figure 5.- Continued.

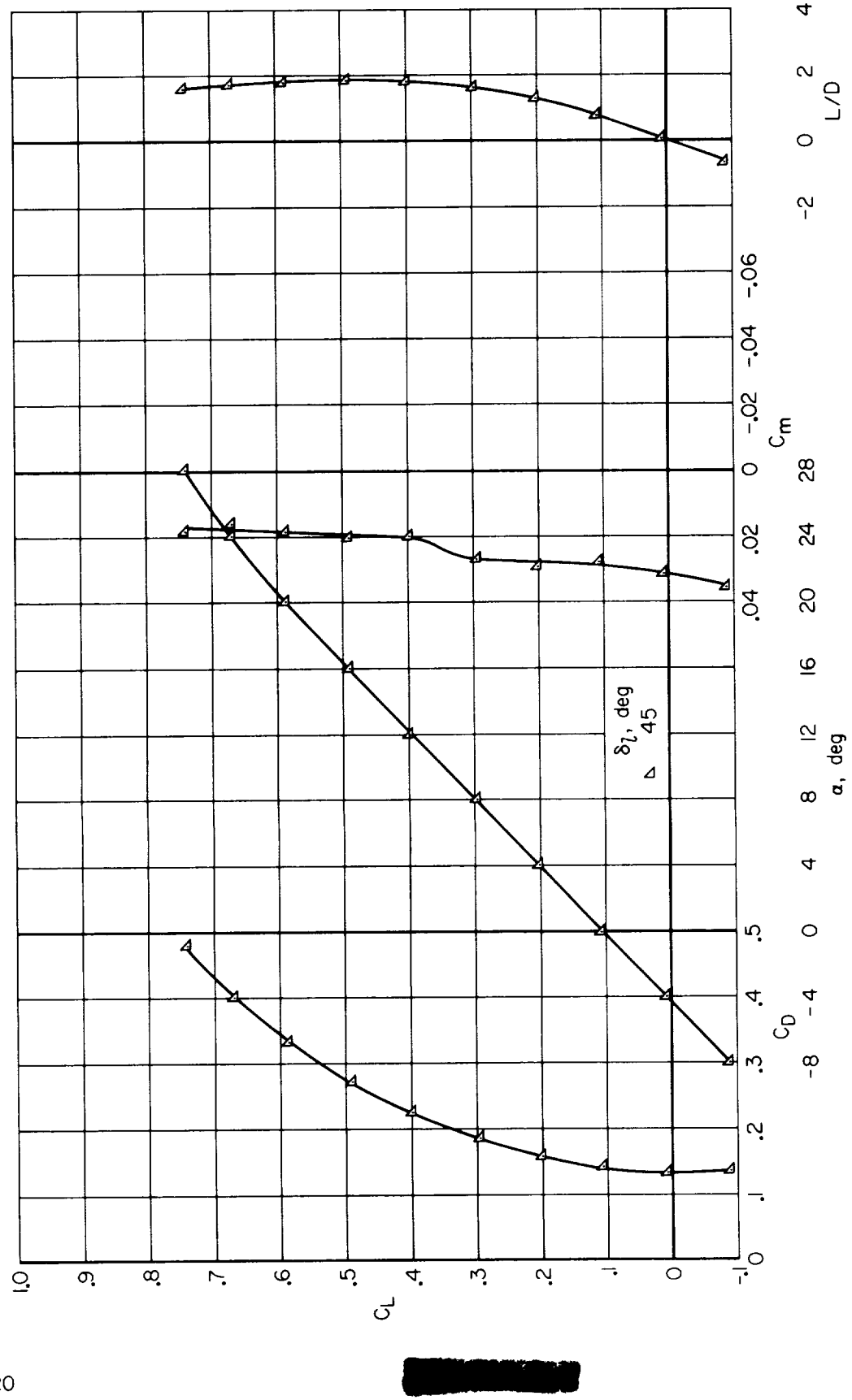

(f) $\delta_u = -35°$

Figure 5.- Concluded.

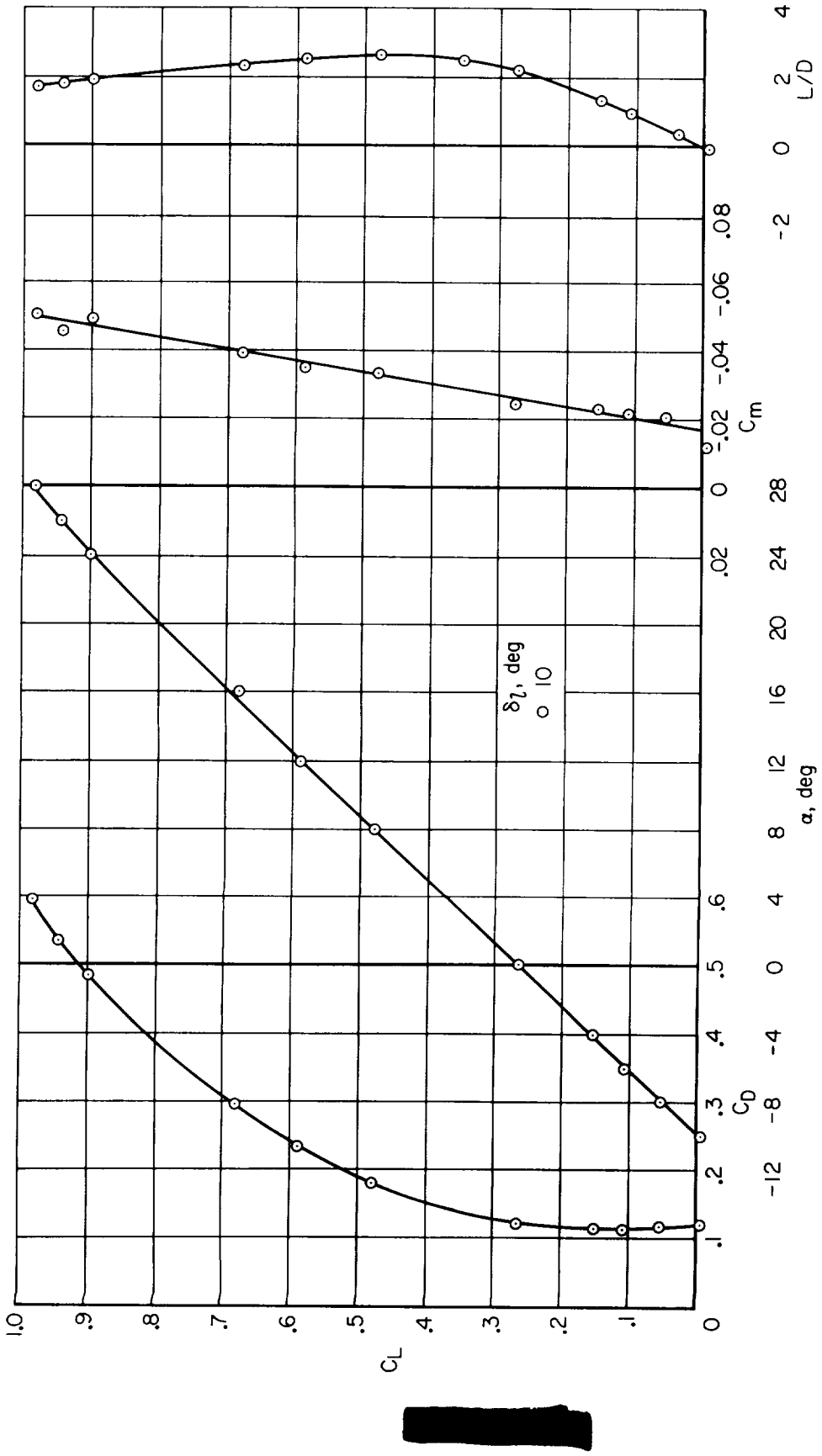

(a) $\delta_u = 0^\circ$

Figure 6.- Longitudinal aerodynamic characteristics for several control settings with the landing gear down.

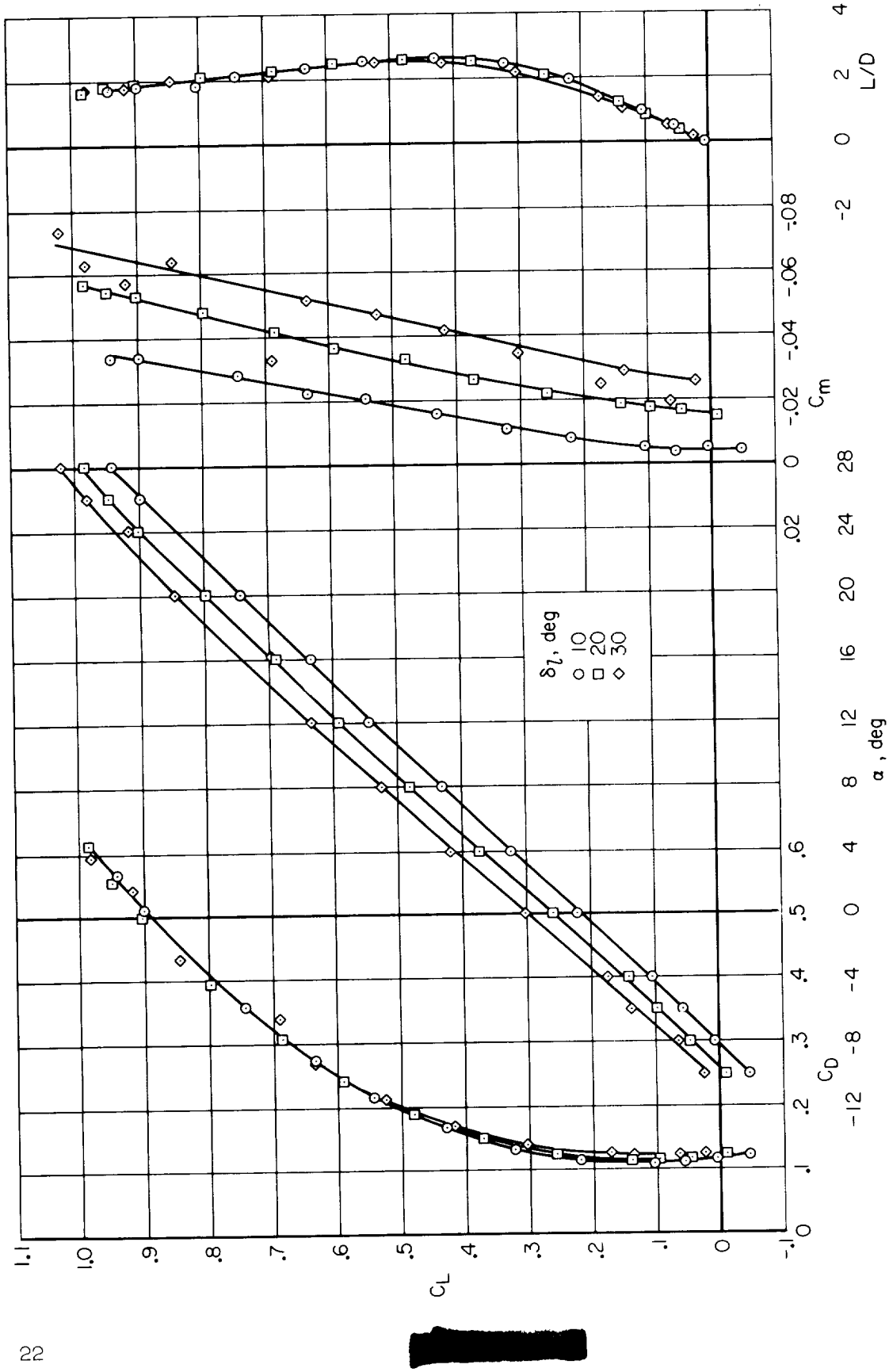

(b) $\delta_u = -5^\circ$

Figure 6.- Continued.

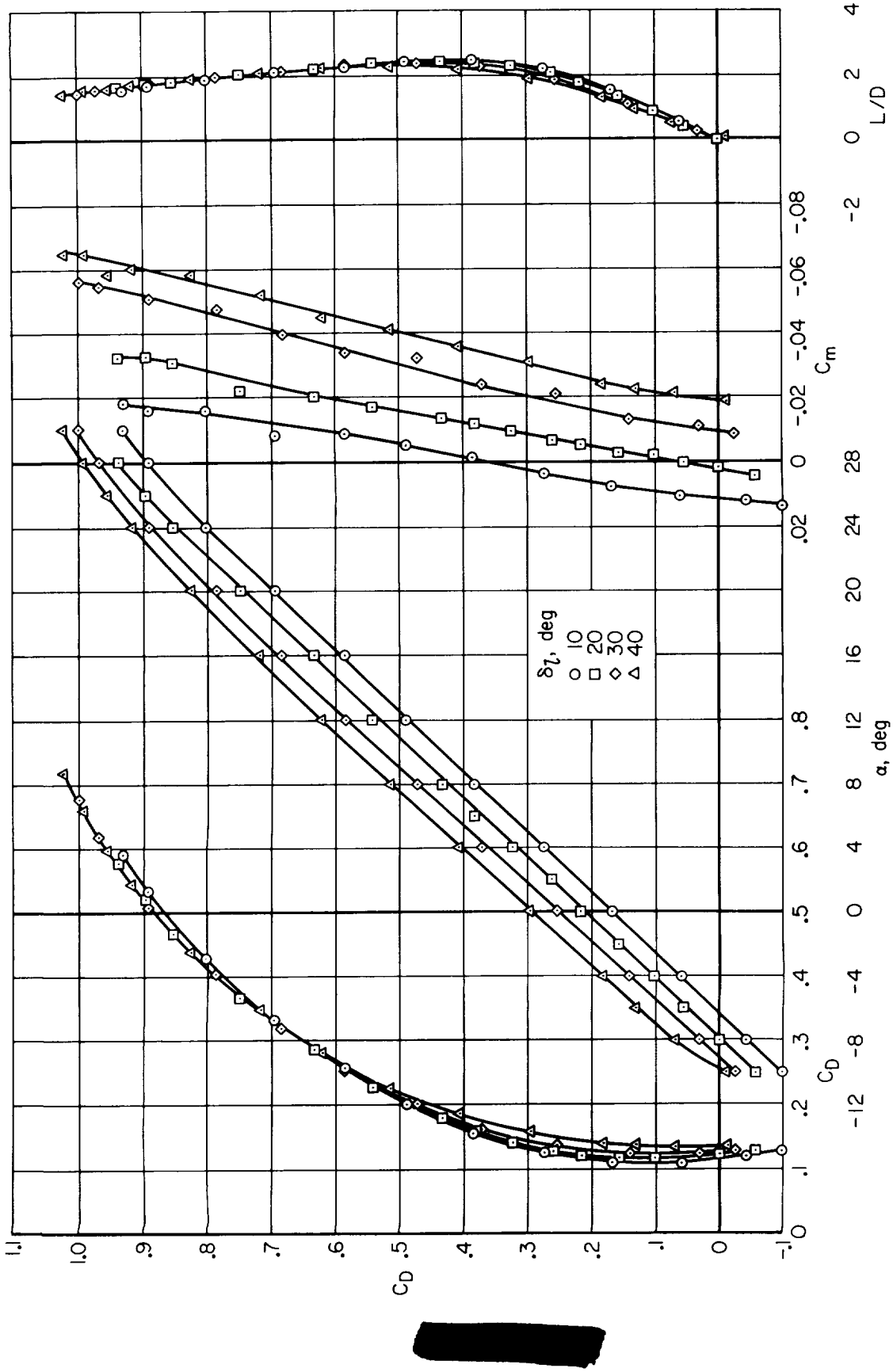

(c) $\delta_{l_i} = -10^\circ$

Figure 6.- Continued.

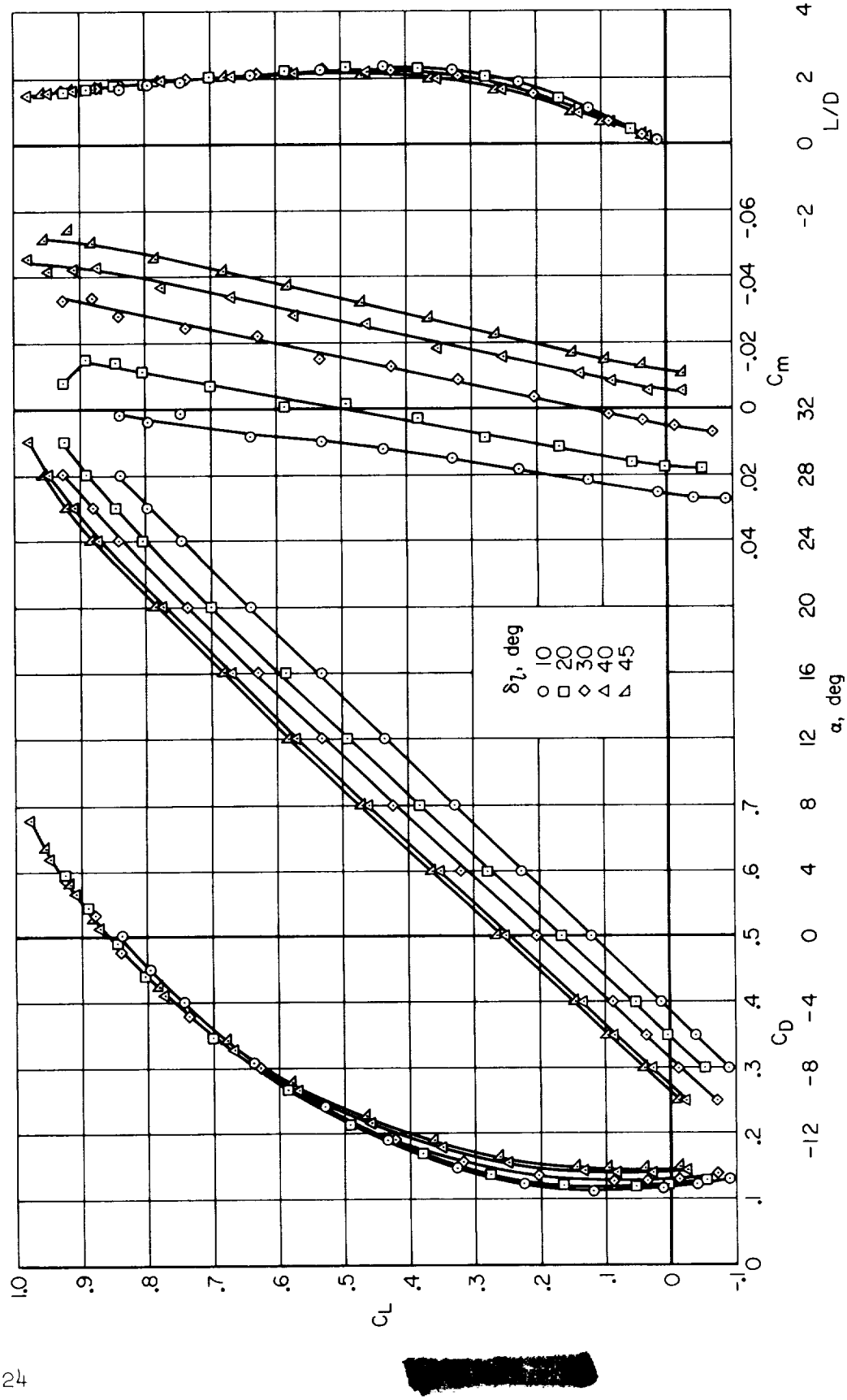

(d) $\delta_u = -15^\circ$

Figure 6.- Continued.

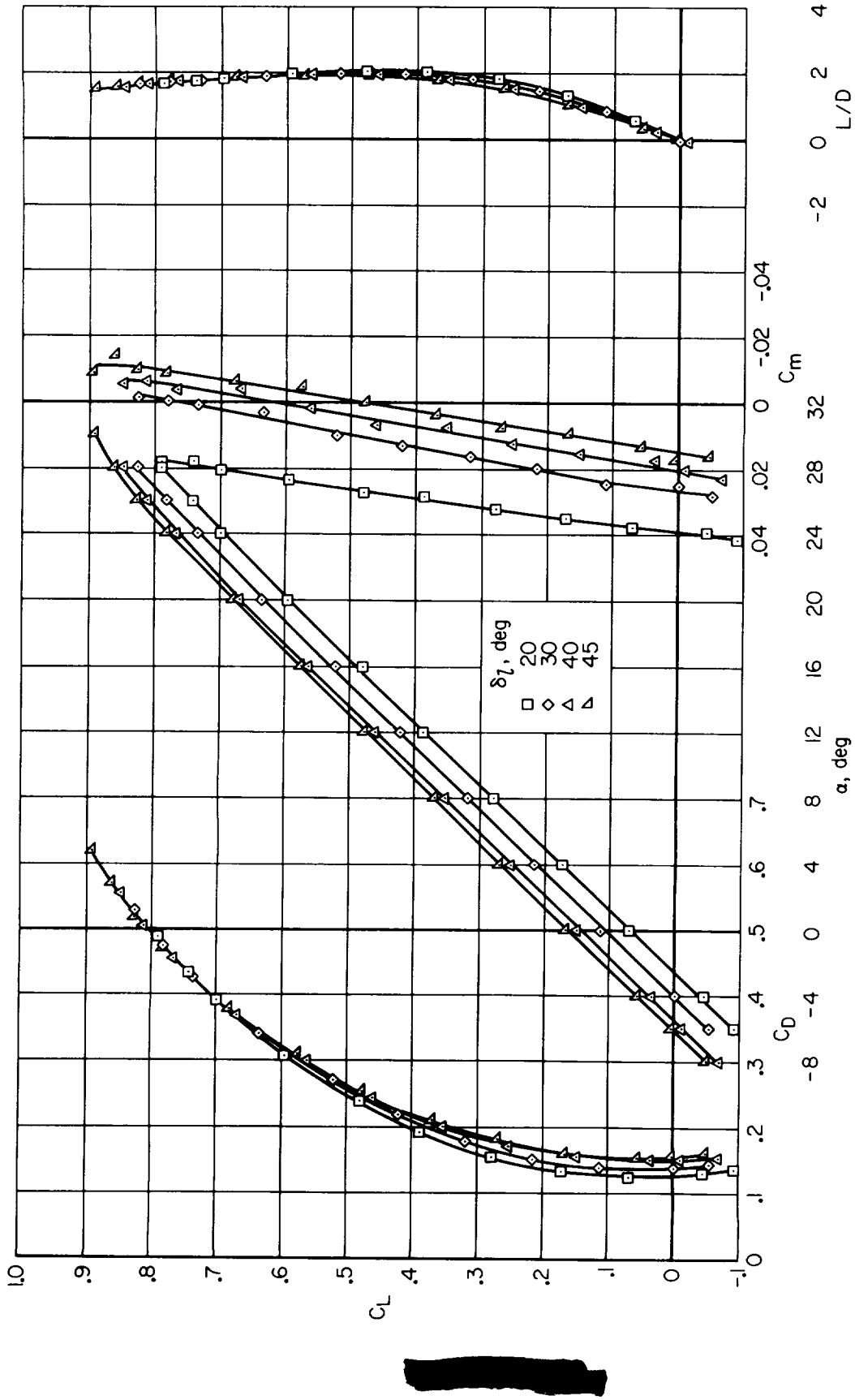

(e) $\delta_u = -25^\circ$

Figure 6.- Concluded.

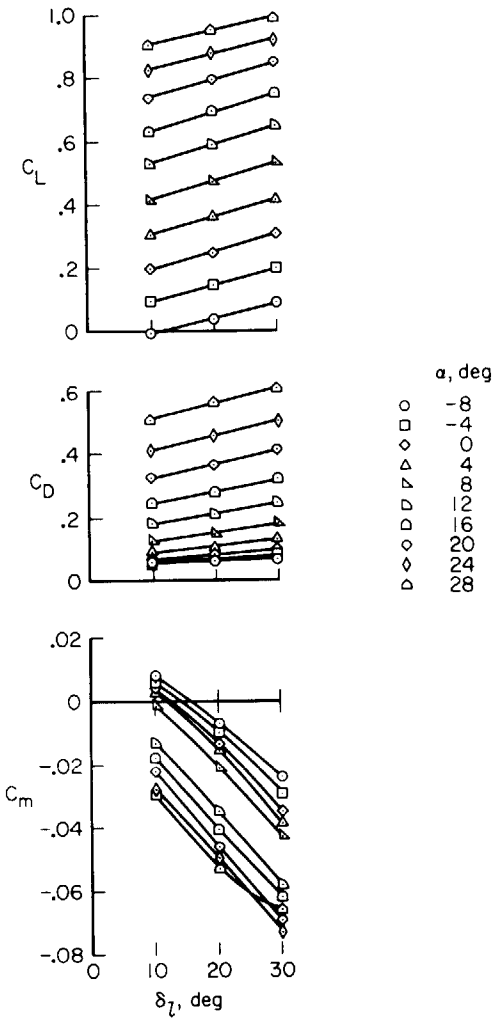

(a) $\delta_u = -5^\circ$

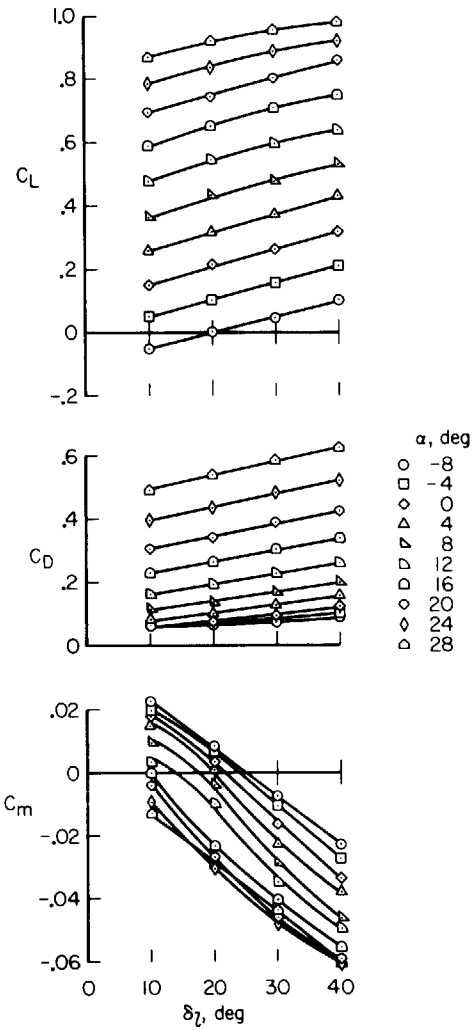

(b) $\delta_u = -10^\circ$

Figure 7.- Longitudinal aerodynamic characteristics as functions of lower flap deflection with the landing gear up.

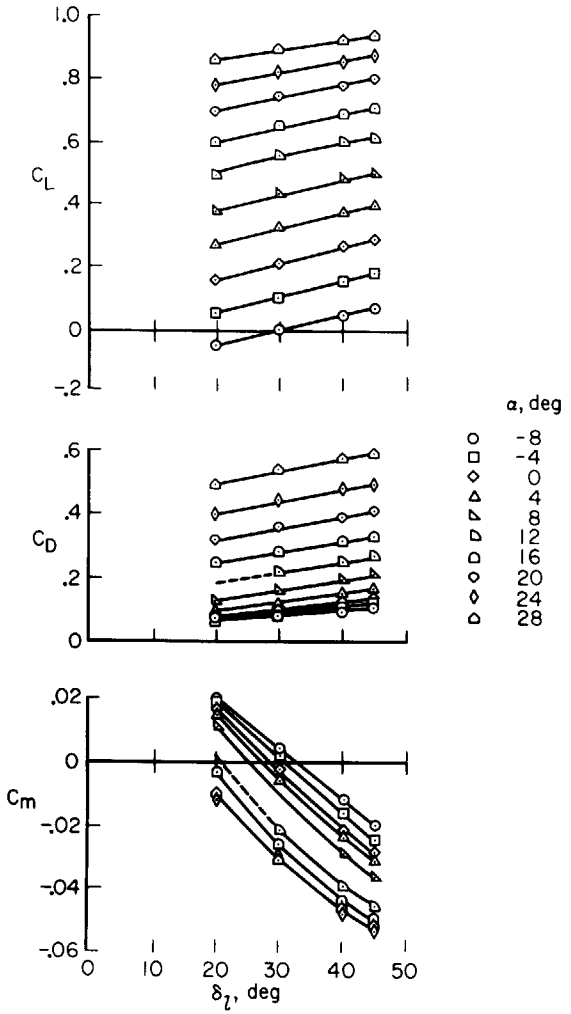

(c) $\delta_u = -15^\circ$

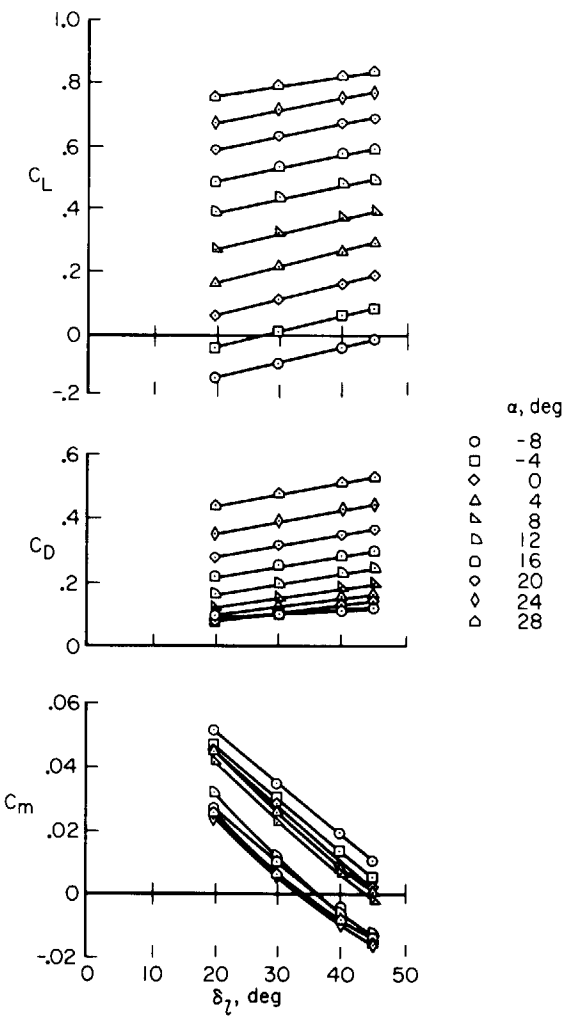

(d) $\delta_u = -25^\circ$

Figure 7.- Concluded.

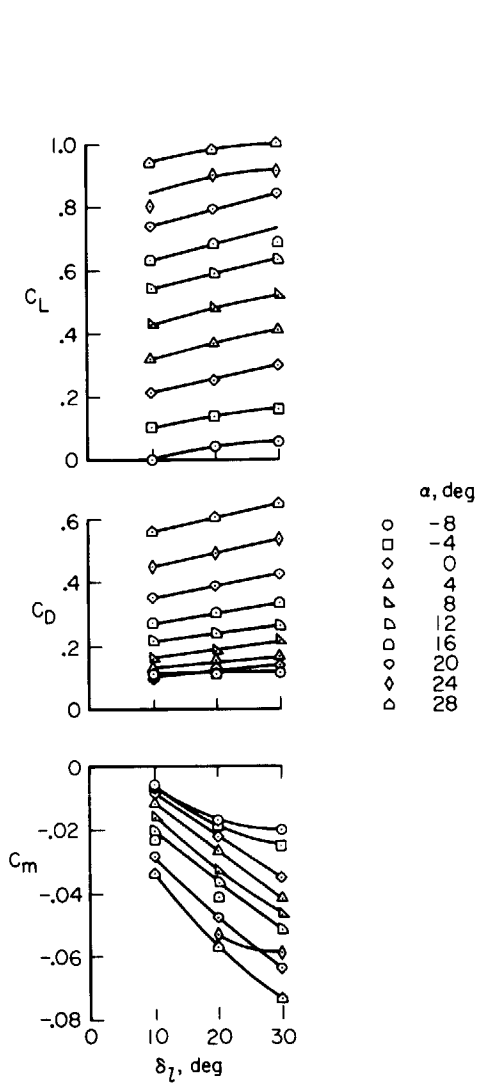

(a) $\delta_u = -5^\circ$

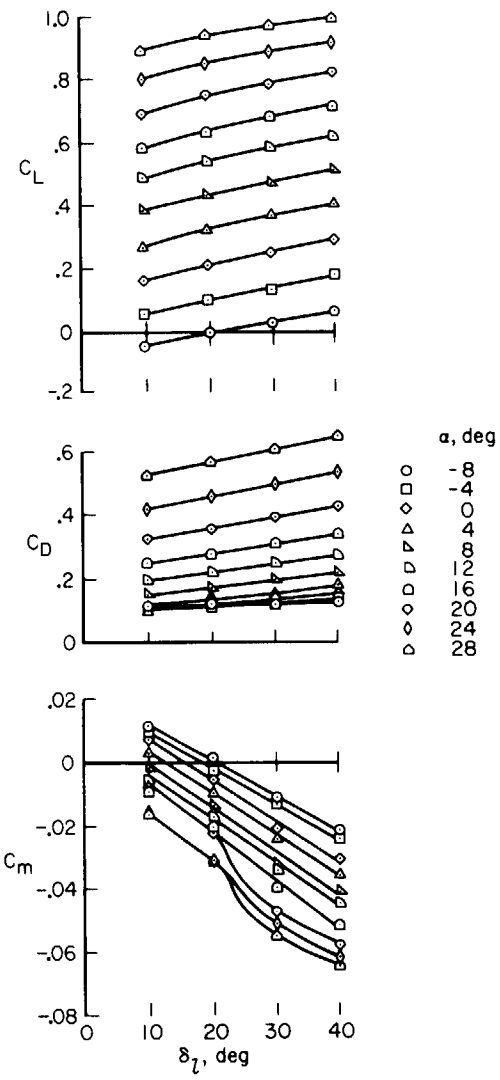

(b) $\delta_u = -10^\circ$

Figure 8.- Longitudinal aerodynamic characteristics as functions of lower flap deflection with the landing gear down.

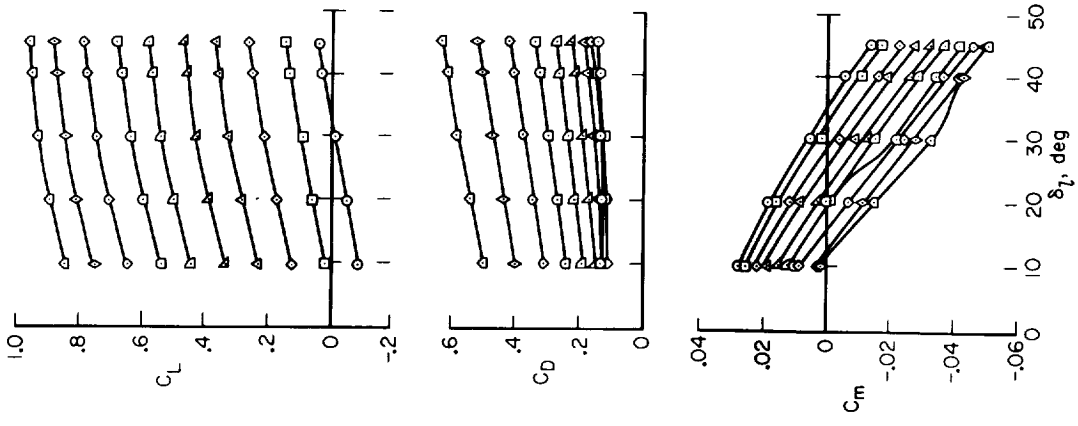

(c) $\delta_u = -15^\circ$

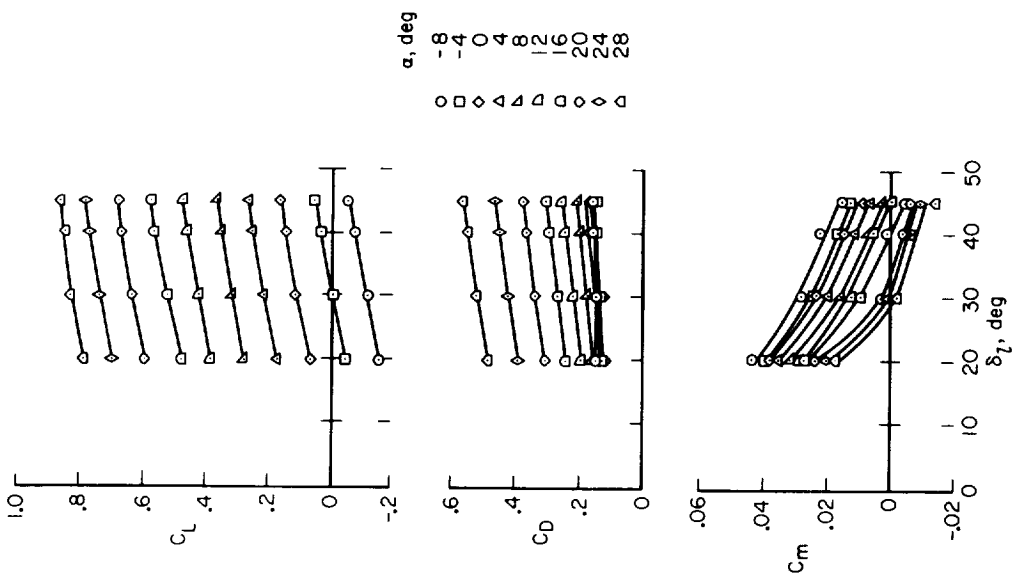

(d) $\delta_u = -25^\circ$

Figure 8.- Concluded.

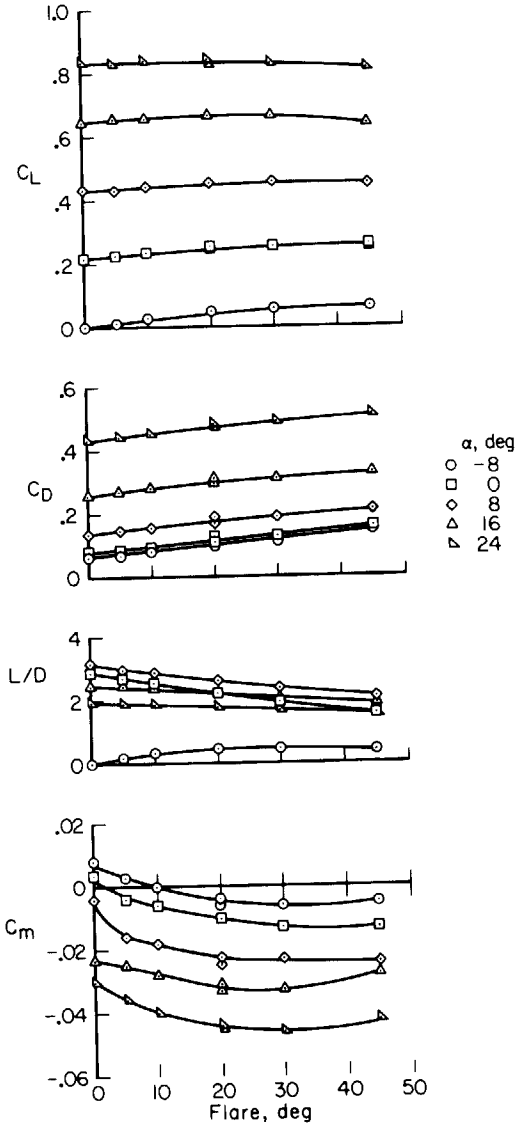

(a) Landing gear up.

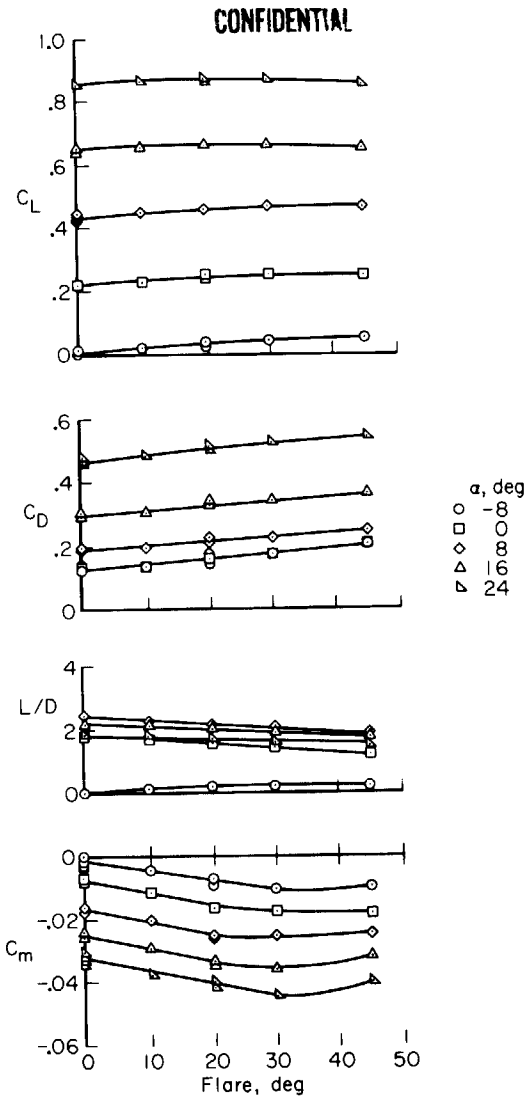

(b) Landing gear down.

Figure 9.- Effect of rudder flare on longitudinal aerodynamic characteristics; $\delta_u = -10^\circ$, $\delta_l = 20^\circ$.

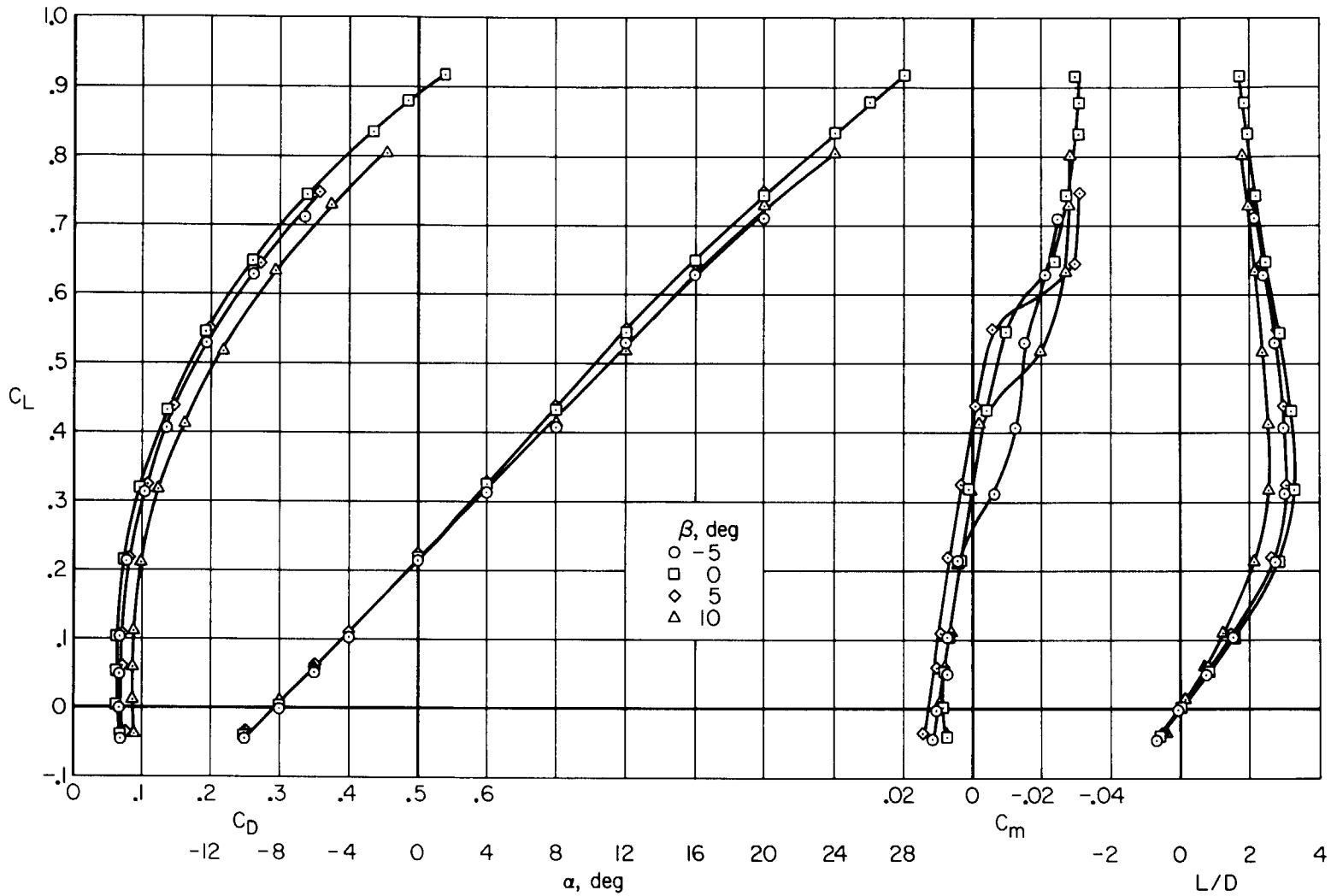

(a) Landing gear up.

Figure 10.- Effect of sideslip on longitudinal aerodynamic characteristics; $\delta_u = -10^\circ$, $\delta_l = 20^\circ$.

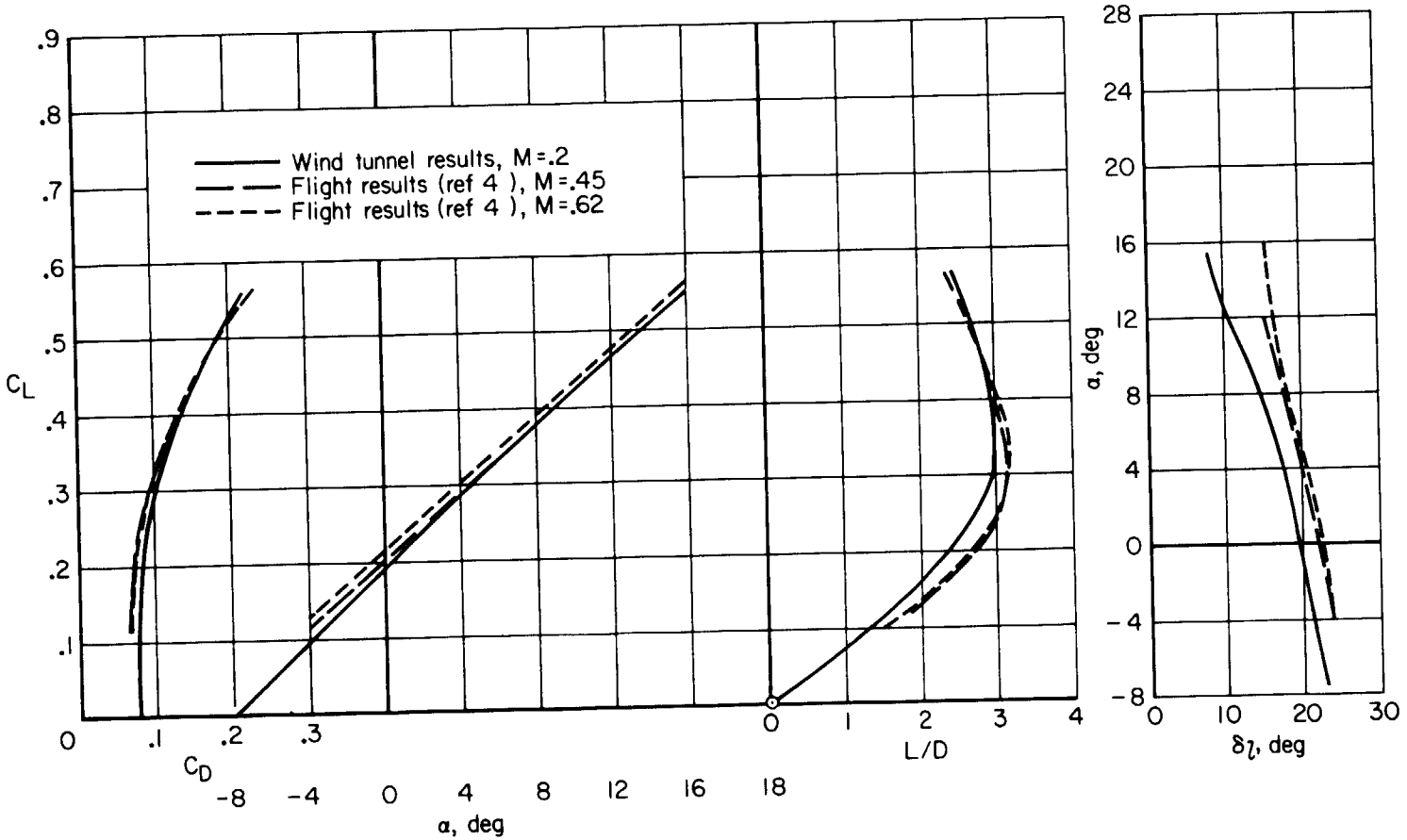

Figure 13.- Comparison of trimmed wind-tunnel results with flight results; 5° rudder flare, δ_u = -11.5°, and moment reference at the 130.5 inch station.

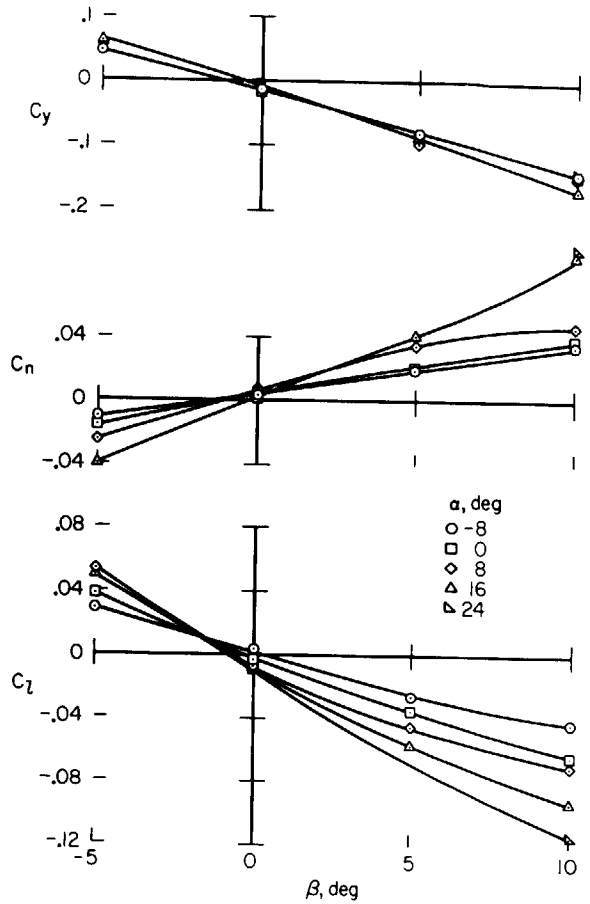

(a) Landing gear up.

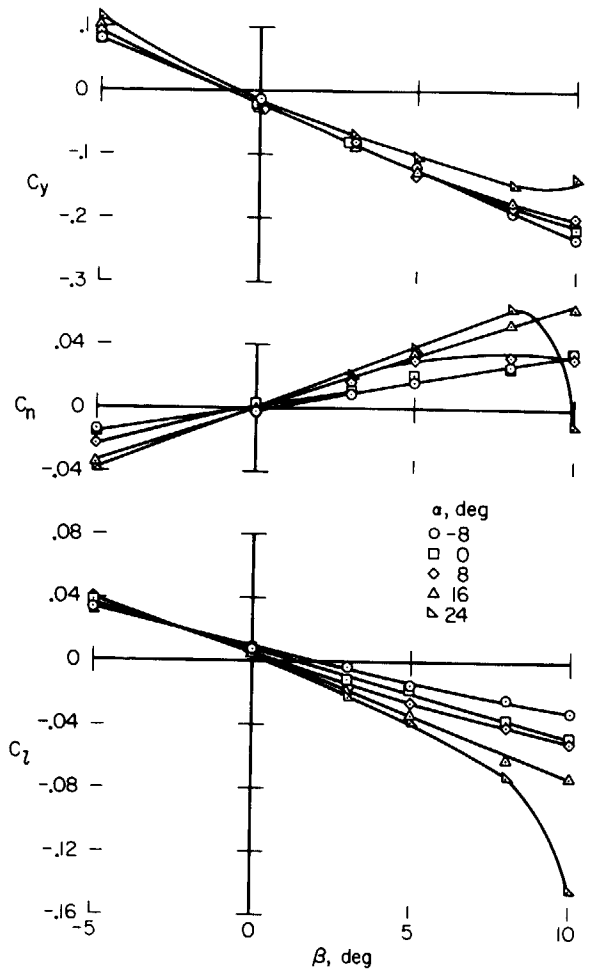

(b) Landing gear down.

Figure 14.- Lateral-directional aerodynamic characteristics; $\delta_u = -10^\circ$, $\delta_l = 20^\circ$.

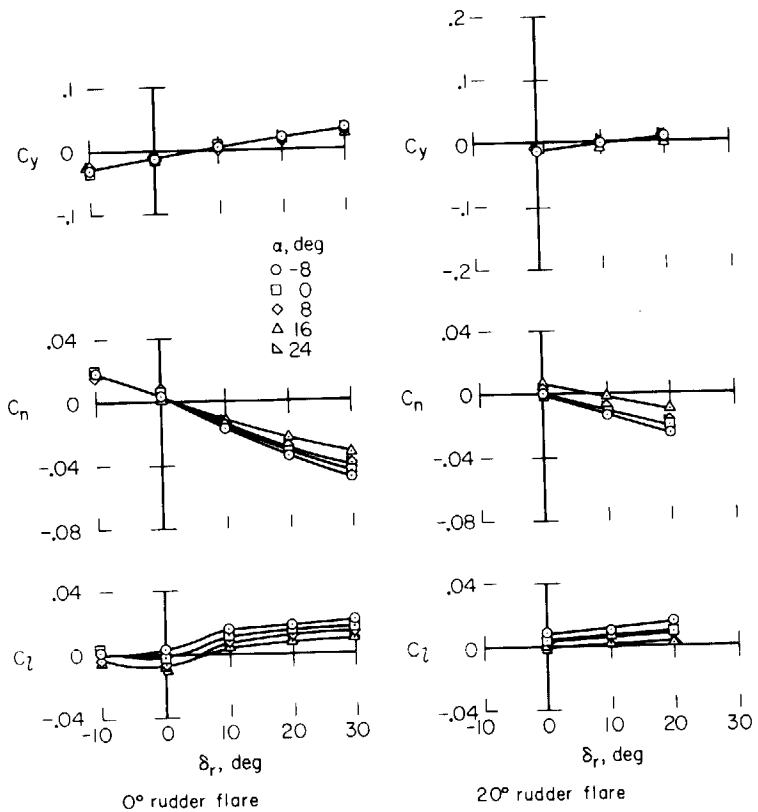

(a) Landing gear up.

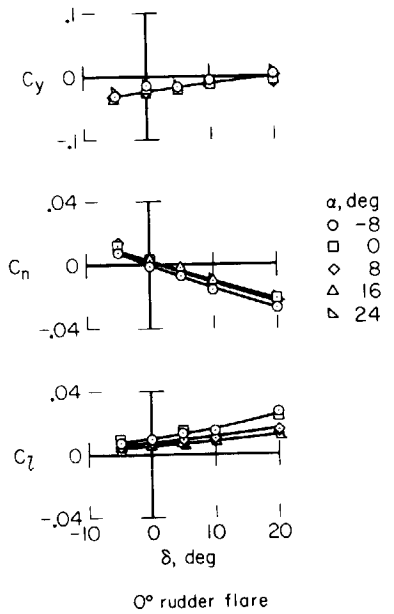

(b) Landing gear down.

Figure 15.- Effect of rudder deflection on lateral-directional aerodynamic characteristics; $\delta_u = -10^\circ$, $\delta_l = 20^\circ$.

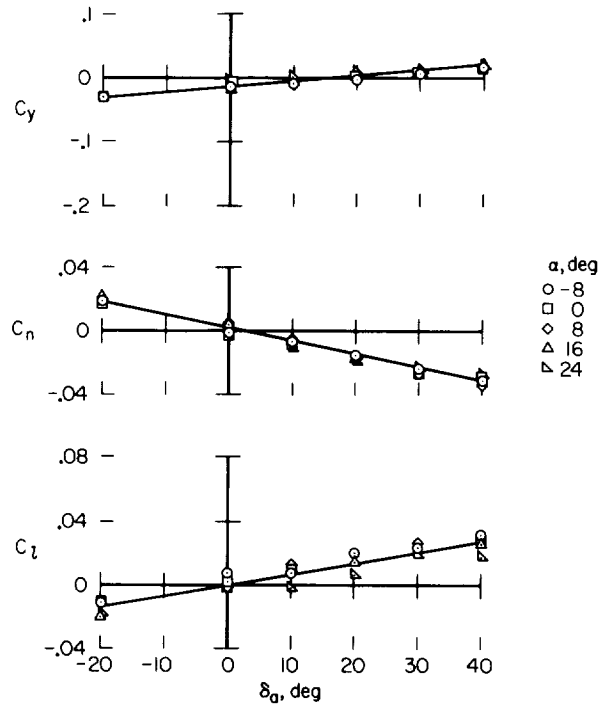

Figure 16.- Effect of aileron deflection on lateral-directional aerodynamic characteristics; landing gear up, $\delta_u = -10^\circ$, $\delta_l = 20^\circ$.